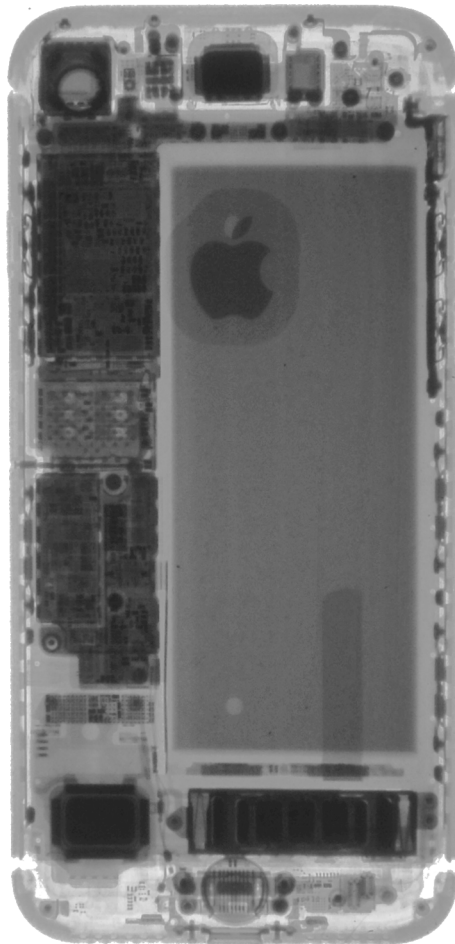# UNIVERSIDAD DE GRANADA

Trabajo Fin de Grado de Física

Design and Development of an X-Ray Machine

Francisco Piernas Díaz

June 2019

Abstract

Este documento reúne el diseño, investigación, construcción y puesta en funcionamiento de una fuente de rayos X para radiografía y escáner TAC de objetos pequeños, utilizando un inversor "Zero Voltage Switching" mejorado, un programa para simularlo, el código para generar radiografías en falso color y un algoritmo de reconstrucción tomográfica. La seguridad en este proyecto es clave debido a la radiación ionizante.

Contents

1   Introduction

The X-Ray analysis has developed constantly over time since Wilhelm Röntgen discovered it's applications. X-Rays are now used not only for simple radiography. Modern algorithms are capable of reconstruct a three dimensional view of the object, allowing us to recover important information about the inside of the object to study, for example, a human body. Ionizing radiations like X-Rays have also been used to discover the structure of the DNA thanks to X-Ray diffractometry.

This project aims to explore the technologies of 2D radiography (sections 10 and 11) and 3D tomographic scans (section 12), and for that, a 3D printable machine is designed, built and tested using a long list of software, tools and parts [28]. One of these parts is an improved Zero Voltage Switching (ZVS) Mazzilli driver, optimized for higher frequency (section 2.1.3). The design and testing is done considering safety, as described in section 9. A Geiger counter is used to ensure that the device is safe to operate and that the operator is not exposed.

In addition to the device, three programs written in C++ have been developed. The first one is an original implementation of the inverse Radon transform to perform tomographic reconstructions of the data gathered wih the X-Ray machine and it's explained in appendix A. The second program, found in appendix B, uses an original algorithm for pseudocolor radiography that tries to improve other algorithms that usually saturates the color of the result. The last program is a numerical model of the Mazzilli ZVS transformer driver inside the machine and it provides useful information about the voltages and currents involved depending on some circuit parameters. It's found in appendix C.
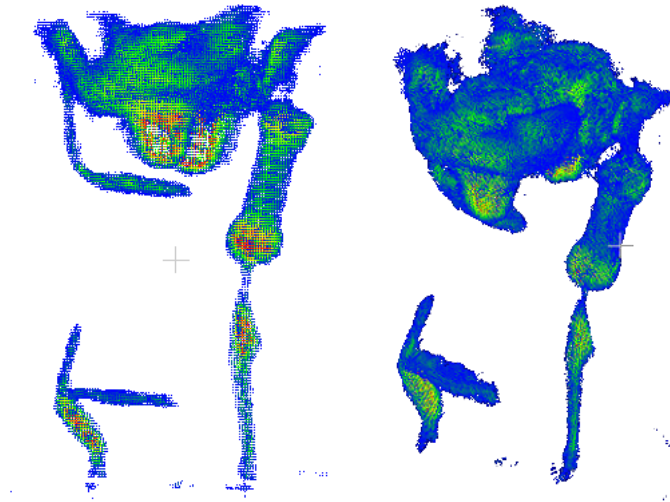

Figure 1: Example of a 3D tomographic reconstruction using the device and software developed in this project.

Part I

Design

X-Rays are considered to have an energy of 1200-120000 eV [24]. In order to make X-Rays, special vacuum tubes are used. These tubes work like a miniature linear electron accelerator. When a high voltage is present, electrons from the cathode travel through vacuum to the anode while accelerated by the potential. When electrons reach the anode, X-Rays are emitted due mainly to sudden deceleration of electrons when they hit the anode.

The most relevant parts in an X-Ray tube are:

- Anode: It contains the target, usually tungsten. Electrons will hit the target and part of their energy will be emitted as X-Rays.

- Cathode: It's usually a heated filament. This makes easier for the electrons to jump to vacuum due to thermoionic effect. In this project it's used a stepdown converter to feed this filament.

- Focusing Cup: Also called grid. It's a piece of metal surrounding the filament that is at less potential than it. This has the effect that the electron beam is narrowed and focused to the tungsten target. It also allows the control of the power of the tube, since it can prevent electrons to jump to the anode.

Figure 2: X-Ray tube used in this project.

The machine of this project uses an X-Ray tube that operates at around 65 kV, so some of the X-Rays obtained will have an energy of roughly 65 keV.

In order to feed the tube with such a high voltage, a special power source has to be designed. There are several ways to do this, and it was chosen to combine a 5.5 kV transformer with a 6-stages voltage multiplier for a voltage of more than 65kV. This part details the design of this high voltage power source and its simulation, the connections of the Arduino controller and the design of the plastic housing.

2   Design of the electric and electronic parts

The machine uses two power supplies. One of them is a 48V power source only used to power the high voltage circuit (ferrite transformer along with it's inverter circuit and voltage multiplier). The second power source is a standard 12V used to power the Arduino board, the fan, the electronic part of the ferrite transformer inverter, the relays and a stepdown converter that lowers voltage to 2.75V for the X-Ray tube filament.

2.1   High voltage source

Some easy to build high voltage power sources use TV flybacks. These transformers work at high potentials (around 20kV) but it's not enough for high energy X-Rays. Using a TV flyback was considered at the beginning of the project since they already have a built-in high voltage secondary, but due to the low power and voltage of these transformers it was finally rejected. It was necessary to design and build a custom ferrite transformer, that can be found in several shapes and types. The type ETD (Economical Transformer Design) was chosen since they are easy to manually wind the primary and secondary. The manufacturer TDK offers it in various sizes. After considering that the desired power of the transformer must be at least 120W, the ferrite transformer ETD59 was finally picked[1] for the task of powering the tube.

The ferrite transformer needs an inverter or driver circuit to work. The easiest solution was a Mazzilli Zero Voltage Switching (ZVS) driver, a DC to AC inverter for the transformer that can self-adjust its working frequency real time so it matches the resonant frequency, almost all power is delivered to the load. Mazzilli ZVS drivers use a center tapped transformer (the primary is divided into two inductors), and two Mosfet transistors that alternately commute at the resonant frequency of the primary-capacitor mesh.
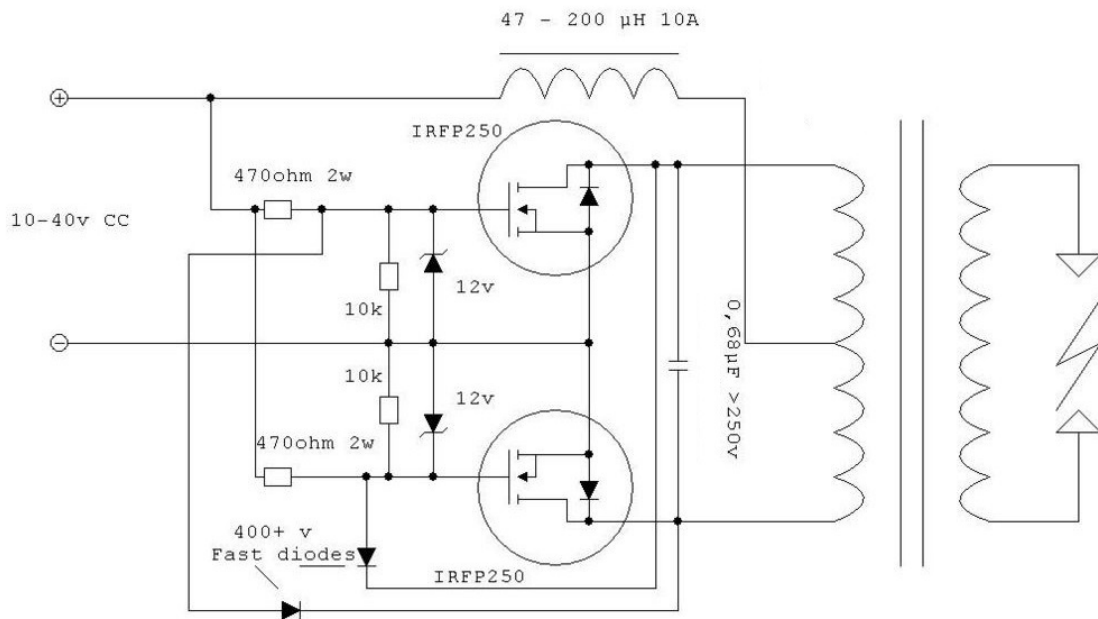

Figure 3: Schematic of the original version of the ZVS Mazzilli driver [3].

2.1.1   Simulation

The software OrCAD was used to simulate the high voltage source: ZVS, ferrite transformer, voltage multiplier and tube, using the alternative version of the Mazzilli ZVS with an extra 12V power supply[2] only to activate the Mosfet gates:

---

[1]The reason of choosing this core is explained in section 2.1.2.
[2]The 12V Zener diodes are no longer necessary since the voltage at gates is already 12V.
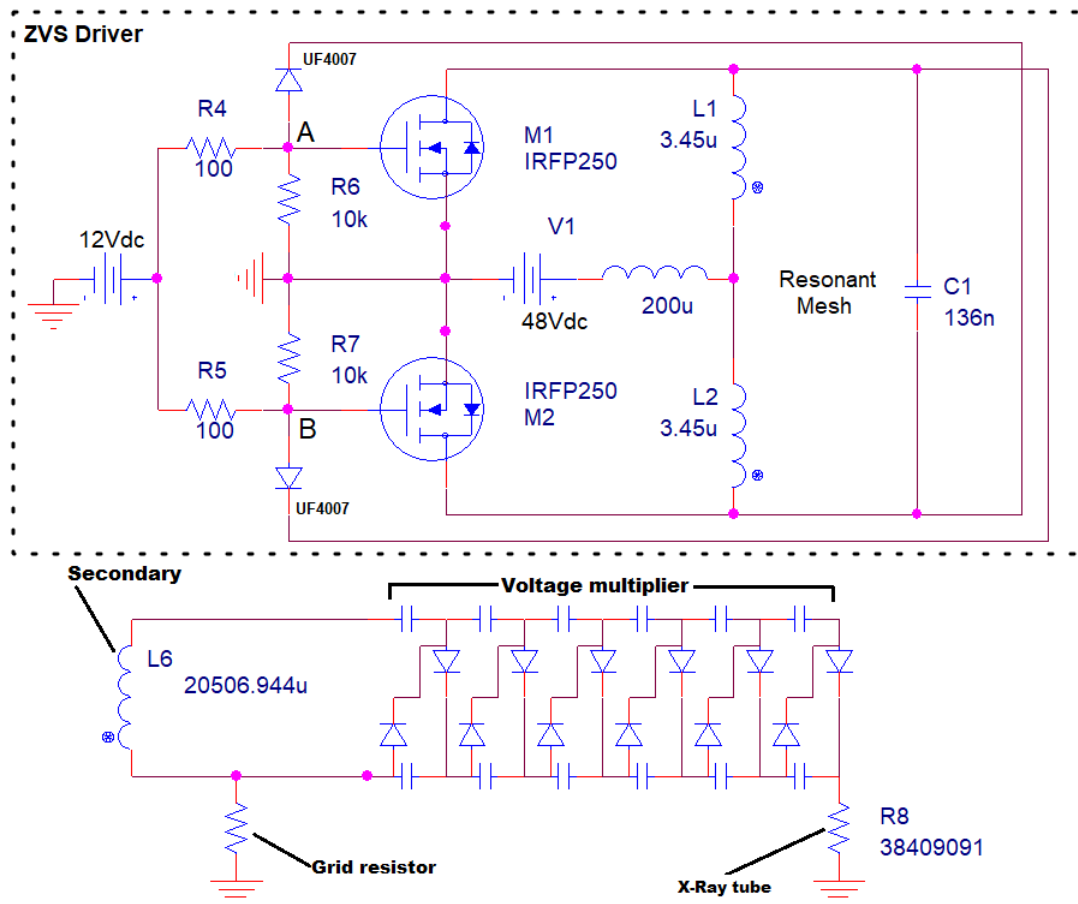
Figure 4: Schematic of the high voltage circuit. Resistor R8 represents the X-Ray tube as an ohmic resistance according to nominal voltages and currents described in the datasheet [2]. Also note that the 470Ω resistors in the original schematic are replaced by 100Ω to improve Mosfet switching speed.

The Mosfets switch at the proper time so the primary (inductors L1 and L2) is resonant with the capacitor C1. Any load connected to the secondary has a reflection at the primary as an impedance inside that resonant mesh (that becomes an RLC mesh). The turning off of the Mosfets is done through two diodes connected to their gates. When the voltage is below 12V after the diode, then voltage at nodes A or B is pulled down and the gate is discharged, turning off the Mosfet. If that voltage is greater than 12V, then the diode blocks current and the gate can charge through R5 or R4, turning on the Mosfet. This is how the circuit manages to turn on and off the Mosfets itself without a controller.

The values for capacitor C1 and inductors L1 and L2 (primary) are the most important parameters of a ZVS. The circuit will work at a frequency that matches the resonant of that capacitor and primary. It was very difficult to choose these values, because:

- Smaller values for the capacitor and primary means higher working frequency, which reduces the primary current, but it also makes the switching harder for the mosfets since they will have less time to switch

- More turns of primary reduces current and frequency, but more turns will be needed in the secondary in order to have the desired voltage.

After several simulations, the 1.5mm gapped version of the ETD59 ferrite transformer was picked. A gapped core is less prone to magnetic saturation. See transformer design 2.1.2. After choosing this ferrite core, these values were finally taken:

- For the primary: 3.45uH each half. This is three turns around the ferrite core for each half (a total of six turns for the primary). For the secondary, 20507uH: 232 turns around the ferrite core.

- C1 capacitor: two 68nF high voltage capacitors in parallel for a total of 136nF.

- Multiplier: six capacitor-diode pairs to multiply the secondary voltage 12 times.

- Mosfets: N-Channel 200V IRFP250N.

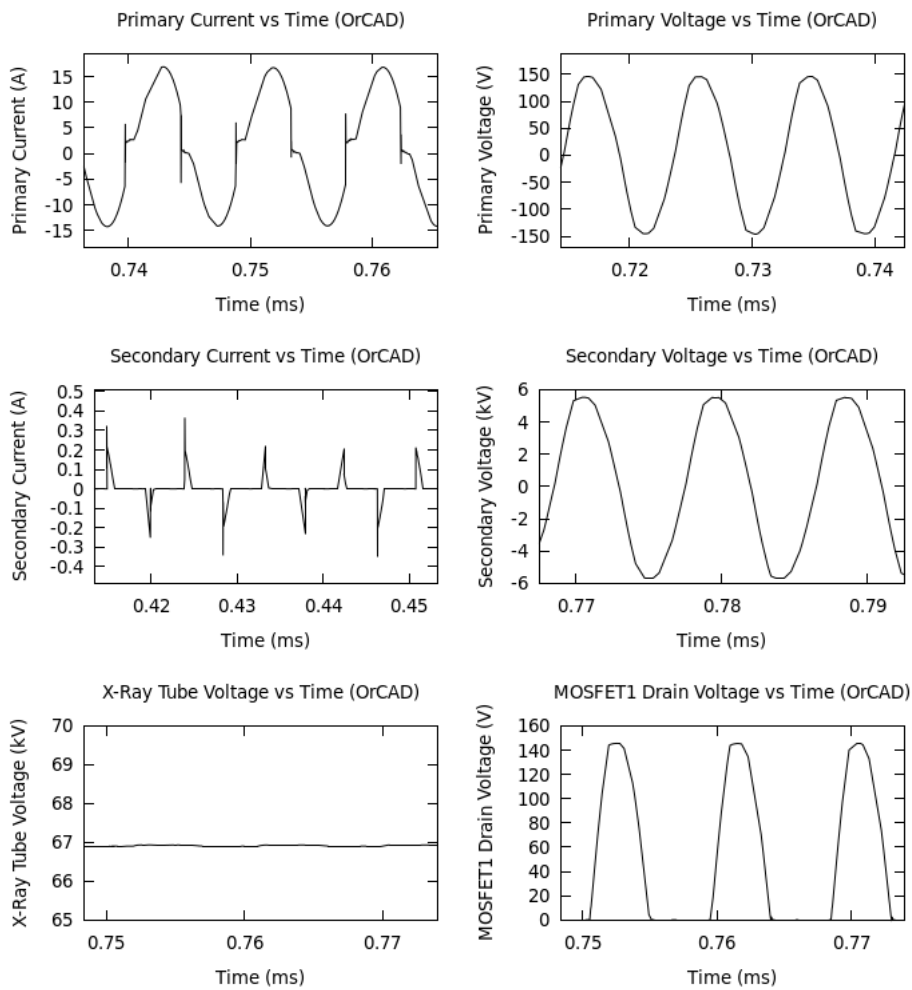The simulation of the circuit gave the following valid results:

Figure 5: Results of the simulation with OrCAD. Note that time is not an important parameter here because the simulation is done considering the circuit already in steady state. Voltages, currents, wave shapes and frequencies are the important information.

2.1.2   The high voltage transformer

In section 2.1.1 it is pointed out that the chosen core was the ETD59. The reason of picking this core is that it is big enough to prevent saturation.
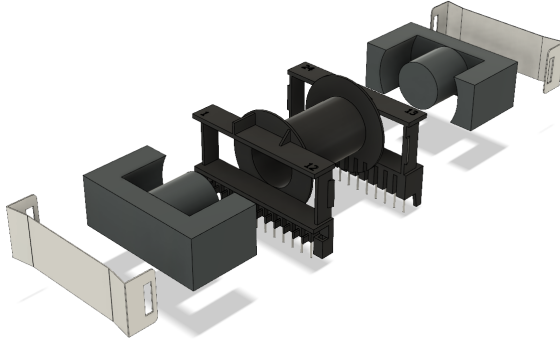

Figure 6: ETD59 disassembly, with yokes, ferrite cores and coil former.

It is very important that we make the transformer work far from saturation[3], it's needed to know the flux density B inside the transformer. A model of a real transformer with no leakage flux or wire resistance but with finite primary inductance and core losses is given by figure 7 [26].

In this model, I_0 is the total primary current, I_c is the current due to core losses R_c, I_1 is the ideal primary current given by $I_1 = \frac{N_2}{N_1} I_2$ and I_m is the magnetizing current in the real primary L_p that creates the flux in the core. The flux density is then given by the following equation [25]:

$$B = \frac{V_p}{N_p \omega A_e} = \frac{150V}{6 \cdot 2\pi \cdot 1.1 \cdot 10^5 Hz \cdot 3.68 \cdot 10^{-4} m^2} = 98mT \qquad (2.1)$$

where A_e is the equivalent cross section of the core [4]. The datasheet also tells us that the saturation density B_s is 320mT, so we are safe working with 6 turns of primary and 150V and this justifies the election of the ETD59 transformer over other smaller alternatives that could result in saturation.
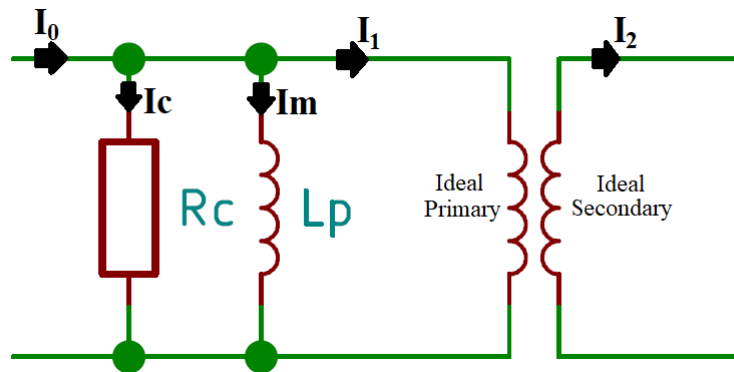

Figure 7: Simplified equivalent circuit of a real transformer.

Regarding losses due to hysteresis and Eddy current, this information is not found in the datasheet of the core but in the datasheet of the material [6]. Figure 8 gives the information needed.

---

[3]The more the flux approaches to saturation, the more the losses by hysteresis will be.

We see that for a flux density of $98mT \approx 100mT$ and $110kHz \approx 100kHz$, we can expect losses of about $150kW/m^3$. According to the datasheet, the ferrite core has a volume of $51200mm^3$, so we can expect that the losses are $P_V = 150\frac{kW}{m^3} \cdot 51200 \cdot 10^{-9}m^3 = 7.7W$, that is an acceptable value.

So far we know that the transformer will have a center tapped primary of 6 turns, a 232 turns secondary and that the expected losses make the design viable. The primary will operate at 150V and 17A; the secondary, at 5500V and 25mA RMS[4].

2.1.3   The Zero Voltage Switching driver

Figure 8: Relative core losses vs frequency and flux density [6].

The next step is designing the inverter to power the transformer (Mazzilli driver). One of these drivers was bought and tested using the transformer with no secondary, performing these modifications:

- The capacitors of the circuit were replaced by two 68nF in parallel so it now has a 136nF capacitance, as designed.

- Cheap ZVS drivers use the same voltage source for the resonant circuit to also power the Mosfets (see figure 3), this was changed so another 12V power source is only used to power the Mosfets. The circuit is now the same as in figure 4.

This first version of the driver (figure 9) worked well for twelve seconds, then both Mosfets burned. The reason is that the gate resistors (those placed at the gate of the Mosfets) have a value of 100Ω (figure 4). This value resulted to be too big, the gate takes very long to charge and the Mosfets switch slowly and work in the ohmic region[5]. These resistors where changed from 470Ω (figure 3) to 100Ω (figure 4) to avoid this but it was not enough. We can't either lower these resistances too much because we will solve this problem but create a new one: when a Mosfet is off, the UF4007 diode at its gate will conduct current from the 12V power source through these resistances and the diode will heat up[6].

The ZVS burning changed plans, it was necessary to create a new version of the Mazzilli driver, changing the way the Mosfets are turn on and off. The solution was to add a Mosfet driver to the circuit that can provide the current needed to the gates for a fast switching. The first considered was the TC4469. According to its datasheet [8], it's a TTL/CMOS driver with a maximum "logic 0" voltage threshold of 0.8V. The UF4007 also
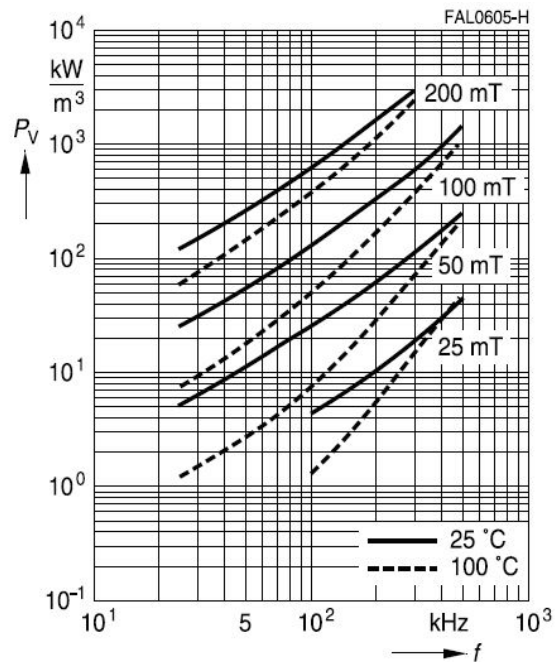
---

[4]Knowing these values will be critical for the construction process.

[5]A half turned on Mosfet acts like a resistor and it heats up quickly.

[6]Also the overall efficiency of the circuit will be low.

have a voltage drop of 0.8V so we can't use[7] a TC4469 and it's necessary to look for a CMOS driver with higher threshold, like the IR2110. It has a threshold proportional to the voltage feeded [9], and it's around 8V when the IR2110 is powered at 12V for a "logic 1" and around 5V for a "logic 0". The fact that there are two thresholds depending if the signal is going from "Low" to "High" or viceversa is called input hysteresis [10] and it's useful to remove false activations or deactivations due to noise.
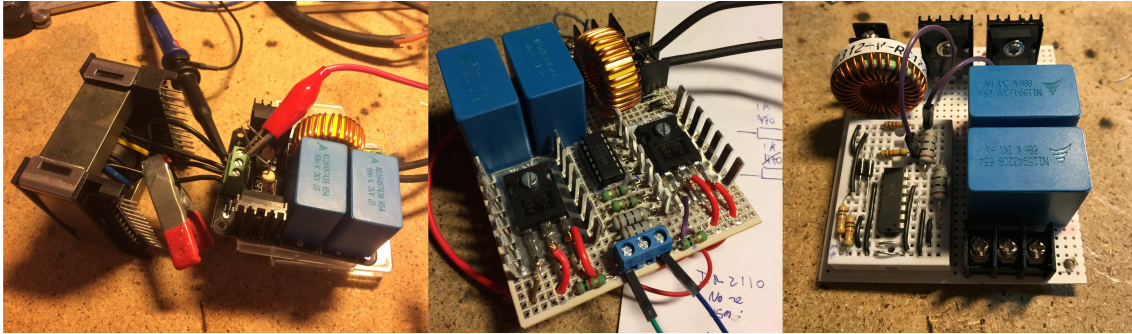

Figure 9: First, second and third version respectively of the ZVS. The second version never worked.

The third version of the ZVS gave bad results. The IR2110's undervoltage lockout (UVLO) shuts down this integrated circuit if the voltage provided is not high enough [11], and this voltage can sometimes go low due to the high working frequency. All these failed versions led to the fourth that worked as expected when the IR2110 was replaced by the TPS2814P[8], that is a bit faster and does not have UVLO.
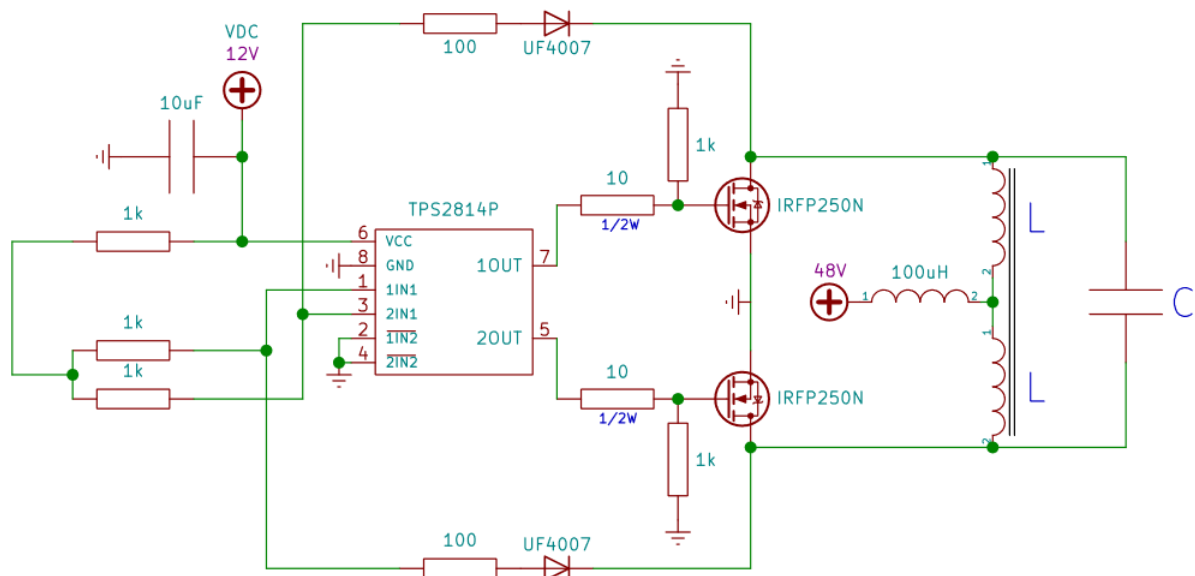

Figure 10: Fourth and final version of the ZVS. The values L and C can be any (not too small), the circuit will work at resonant frequency. For this project, $L = 3.45\mu H$ and $C = 136 nF$.

---

[7]The TC4469 is not an option since the UF4007 can't pull down voltage below the "logic 0" threshold.

[8]Choosing the right full CMOS Mosfet driver took a long time of searching models and reading datasheets.

This schematic has the following key points:

- The addition of a Mosfet driver results in a substantial innovation of the original circuit.

- The power lost through the UF4007 diodes is negligible compared to the original circuit in figure 3.

- The gates of the Mosfets are charged through a 10Ω resistor instead of 470Ω (figure 3) or 100Ω (figure 4), so it switches much faster.

- The 100Ω resistors were added after checking with the oscilloscope that the noise at the inputs of the TPS2814P is smaller when placed. A hypothesis of why this happens is that those resistors delay the turning off process of a Mosfet some nanoseconds (the inputs of the TPS2814P have a small capacitance), giving time for the other Mosfet to turn on.

Although this circuit is very different to the one simulated, the results of the simulation are still valid. This is because we have only improved the turning on and off process of the Mosfets, but no changes were made to the resonant mesh of the circuit.

2.1.4   The high voltage multiplier

At this point we already know how the ZVS and the transformer will be, but these two components only gives us 5.5kV, much less than the 65kV needed. The next step is adding a voltage multiplier:
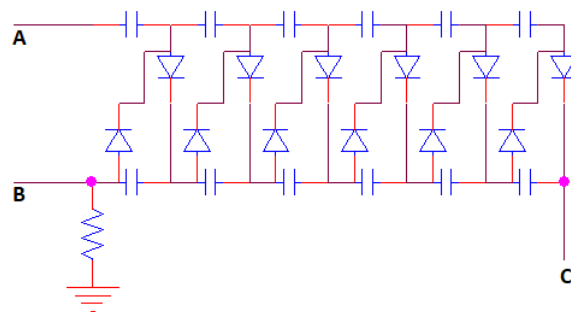

Figure 11: Schematic of the voltage multiplier. A and B are the inputs, C is the output.

When an alternating voltage source is present at inputs A and B (the secondary of the transformer), the diodes commute current in a way that capacitors are charged with a rising potential from left to right in figure 11 and discharged to the load at C (the X-Ray tube). Voltage multipliers can be designed to multiply voltage as many times as needed by just extending the pattern capacitor-diode shown in figure 11. The designed multiplier[9] has 12 capacitors so it will multiply any AC source at the input 12 times and give a high DC output.

---

[9]The resistor shown in figure 11 is the tube's grid resistor to limit power, that has to be put at less potential than the cathode, as explained in the introduction of part I. The cathode (filament) is grounded and this forces current consumed by the tube to pass through that resistor, making terminal B to be in fact at less potential than the filament. The grid is then connected to B and this way the focusing cup is below the potential of the filament.

The highest voltage that the capacitors or the diodes will have to manage is two times the input, so if our input is the secondary of the transformer that is 5.5kV, we have to pick capacitors and diodes capable of handling at least 11kV. Ceramic 1nF 20kV capacitors and ultra fast 20kV 2CL2FM diodes were picked.

2.1.5   The extender

The extender is a small piece inside the machine with the purpose of extending some cables going to the Arduino board. It contains a voltage divider that allows the Arduino board to read the voltage of the filament and a fuse, also for the filament. This is very important because any failure of the stepdown converter that feeds the filament will result in this filament burnt and the X-Ray tube broken without possibility to repair. Arduino reads the voltage and stops everything if the voltage is more than the programmed limit.
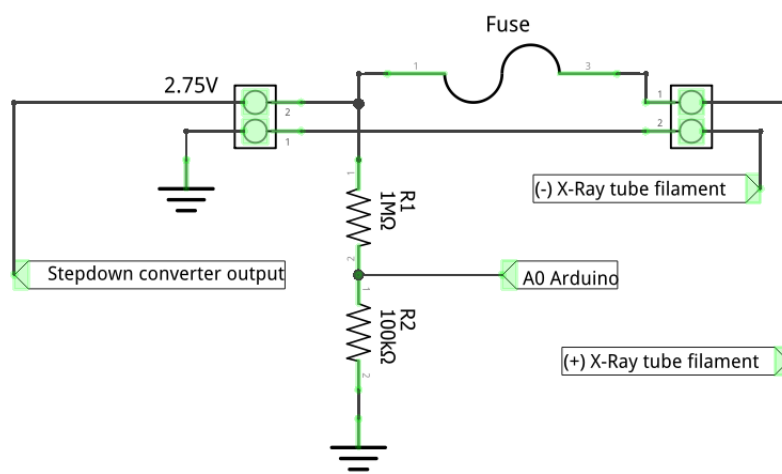

Figure 12: Schematic of the extender.

2.2   The Arduino UNO controller

Everything in the machine is controlled by an Arduino board. The machine has been designed in a way that it performs these tasks:

- It receives commands via USB, allowing a remote control.

- It reads the voltage of the filament via a voltage divider in the extender.

- It manages the buzzer sound and the two lasers separately. It also controls the relays that activate the ZVS and the X-Ray filament.

- It activates the main 48V PSU and receives a signal from it in case something goes wrong.

The PW-ON connection between Arduino and the main 48V PSU allows to activate this power supply via software. On the other hand, the PWG (Power Good) wire is a signal from the power supply to Arduino. When its state is Low, it means that something is wrong [7] (like a shortcircuit) and Arduino stops everything.
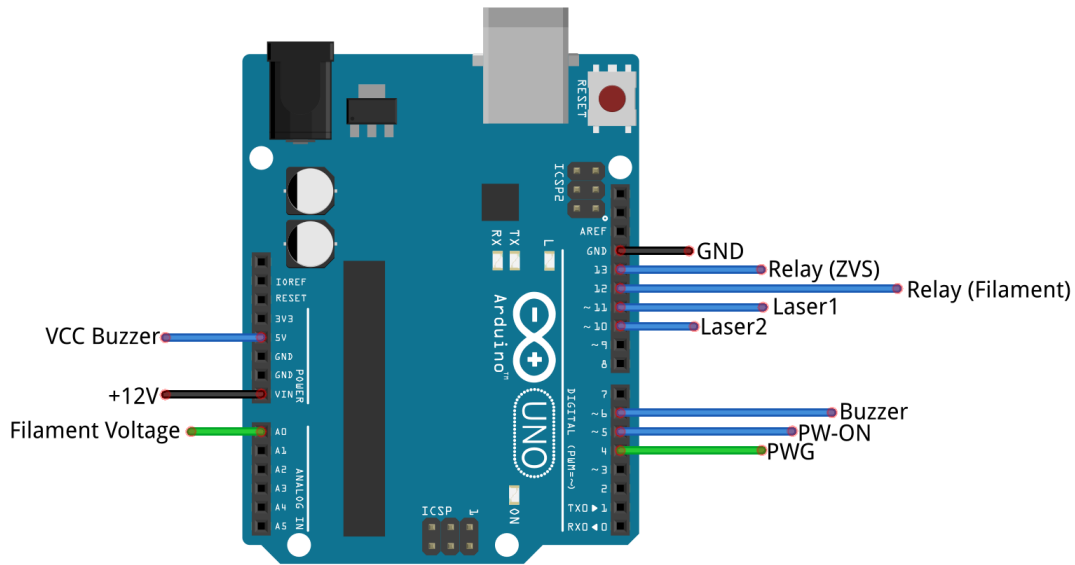
Figure 13: Connection schematic of the Arduino board. Blue wires are outputs, greens are inputs and blacks are supply voltage.

These are the programmed commands:

- E: check machine status (Arduino reads filament voltage and checks the PWG signal of the 48V PSU).

- H+percentage: it sets the brightness in percentage for the horizontal laser. Example: H20 sets it by 20%.

- V+percentaje: the same, but for the vertical laser.

- P: stop everything. If the tube was activated, it stops; if it was counting down to activate, it will stop. The 48V PSU, the filament, the ZVS and the laser grid will be turned off.

- C+integer: it sets the countdown. Example: C10 sets a 10 second countdown when the X-Ray command is sent.

- R+integer: X-ray command. When sent to Arduino, the countdown set by the previous command starts. When it reaches 0, Arduino turns on the 48V PSU, the ZVS and the filament. The machine will X-Ray for as many milliseconds as set by this command. Example: R2000 will X-Ray for 2 seconds.

The activation and deactivation of the machine are done in a very specific way:

- To activate the X-Ray tube: Arduino first activates the 48V power supply and checks that everything is good (just like executing command "E"), then it activates the filament, waits 100ms and activates the ZVS, that immediately starts oscilating and the X-Ray tube is activated. This is done in order to have the tube ready for the high voltage since at the moment the ZVS is activated, the voltage on the tube rises quickly to 65kV.

- To deactivate the X-Ray tube: Arduino first stops the power supply and the filament at the same time, waits 400ms and then it shuts down the ZVS. It's important to first disable the 48V power supply before turning off the ZVS, because this way any energy left in the ZVS can leave the circuit through a fully activated Mosfet. Otherwise a short but high voltage peak will happen at the drains of the Mosfets. At the moment the power supply is turned off, the ZVS starts loosing energy. Only when there is no energy in the ZVS it's safe to turn off the Mosfets.

3   Design of the 3D printed housing

The machine uses a fully 3D printable housing designed from scratch using Autodesk Fusion 360, then sliced with Ultimaker Cura and printed with a BQ Witbox 2. The design was done keeping in mind that:

1. The housing must be small and compact enough to be printed in a BQ Witbox 2, that has a printable surface equivalent to an A4 paper sheet.

2. It must be big enough to accommodate all the pieces of the machine.

3. It has to be designed and printed with all supports and holes already done, so the only thing to do next is assembling.

4. Last but not less important, it has to be elegant.

The design took a very long time of the project since it resulted to be very difficult to put inside that housing all the parts, taking into account that some parts need more cooling than others, some high voltage parts need to be placed far from others, the X-Ray head must have lead shielding, the high voltage cables can't be too close to other pieces, etc. The design started with the idea of putting all the parts in a single level, but soon another level was required.
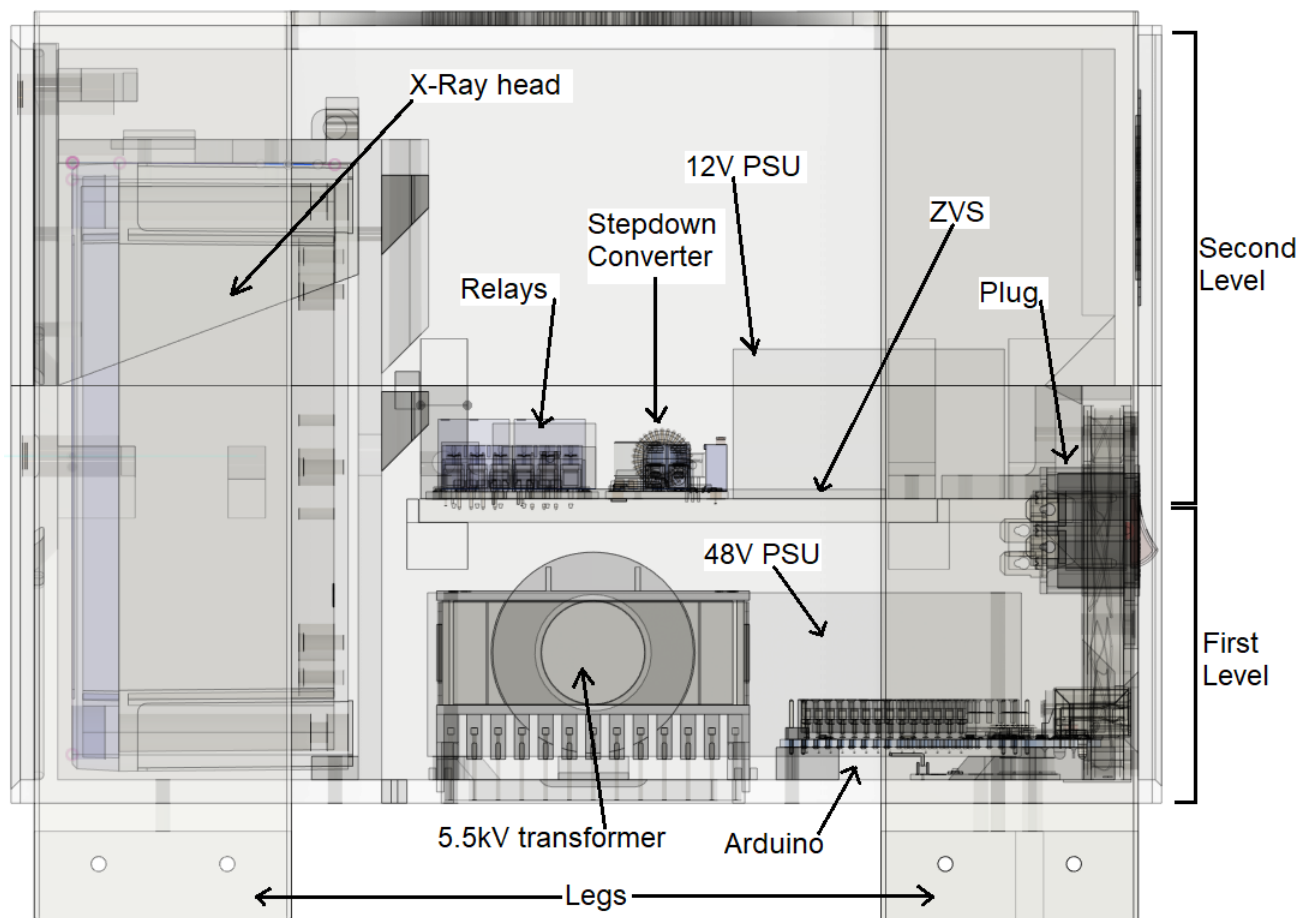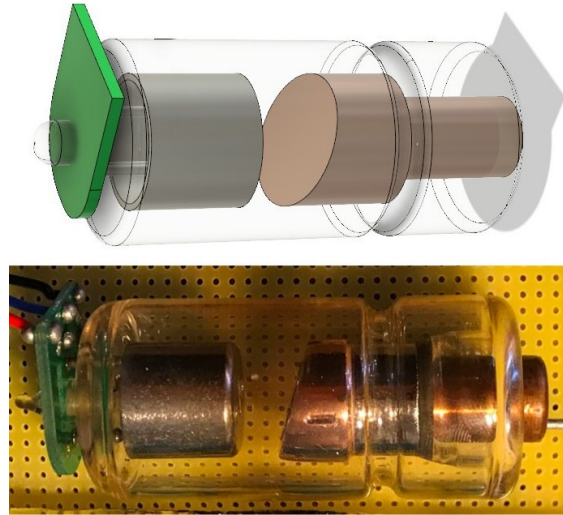

Figure 14: Lateral view.

Figure 15: Some 3D models of parts like the tube were created using just a calipper to measure sizes in order to make the design easier.
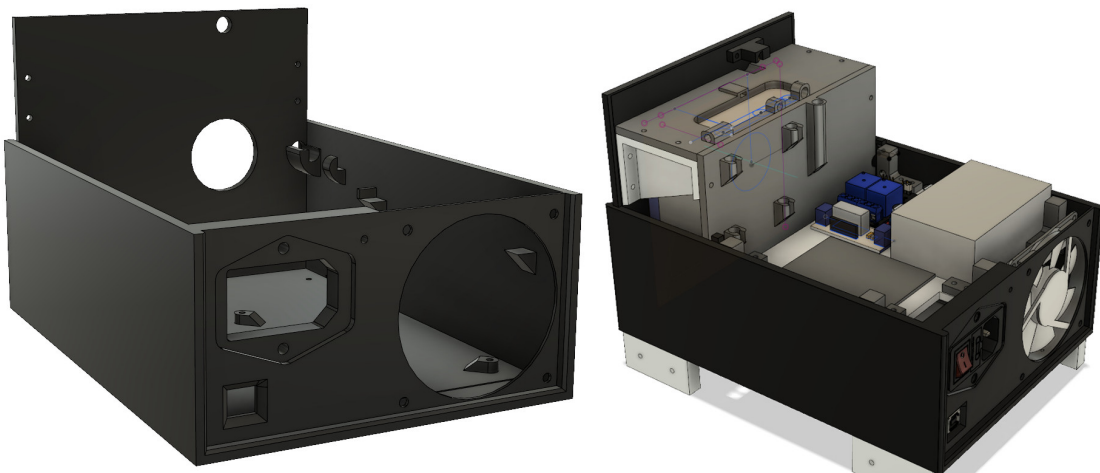

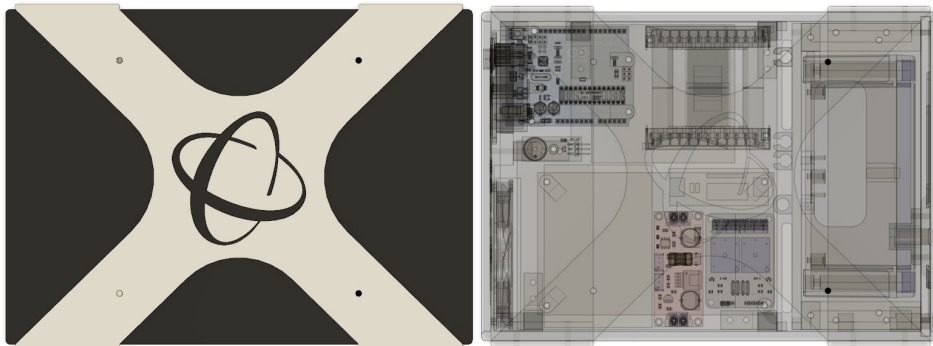Figure 16: View of the bottom part of the housing empty and with parts.

Figure 17: View from top with Facultad de Ciencias de la Universidad de Granada's logo.
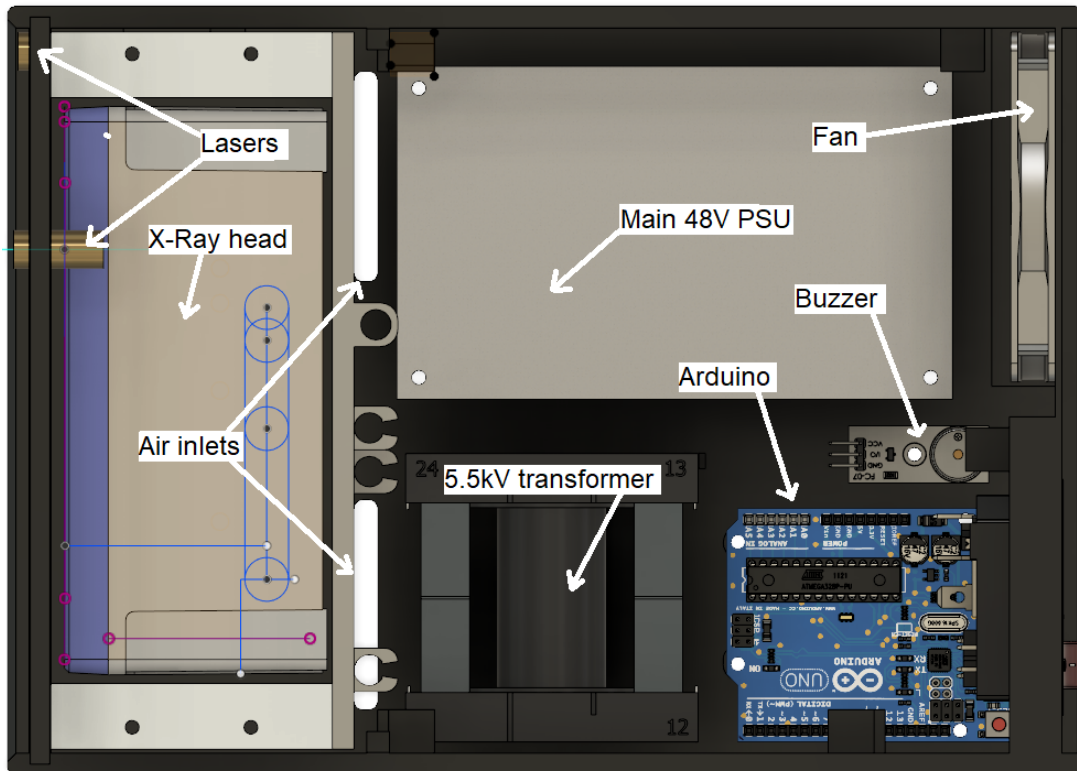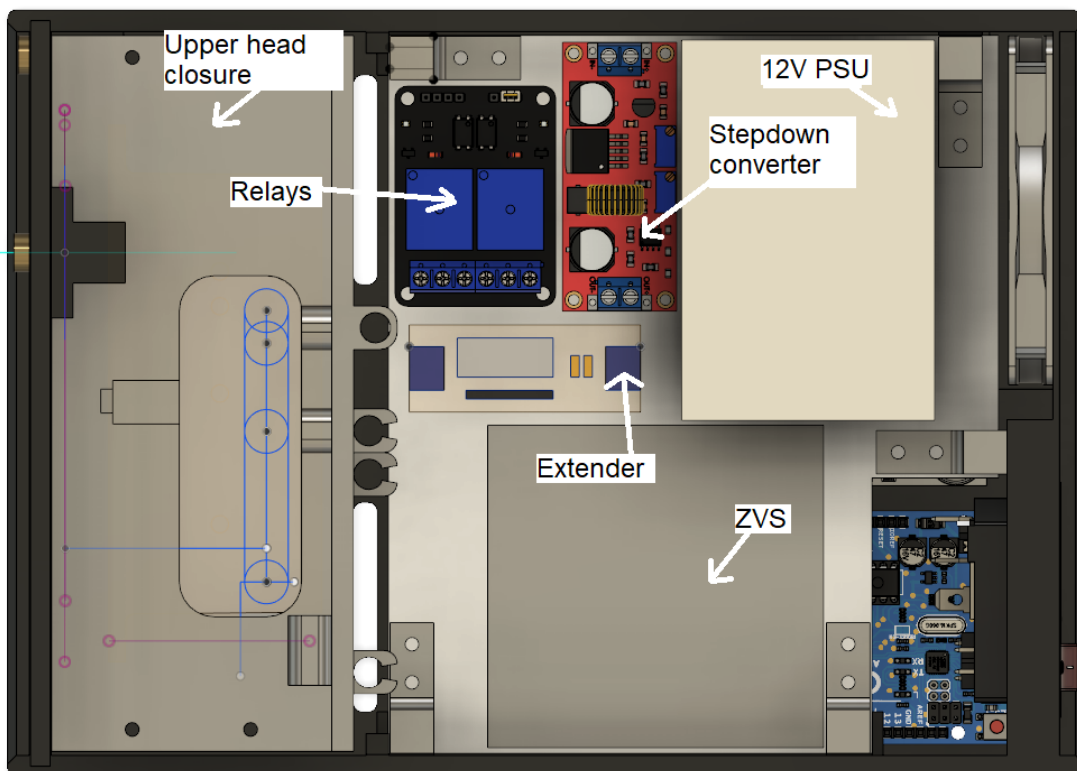
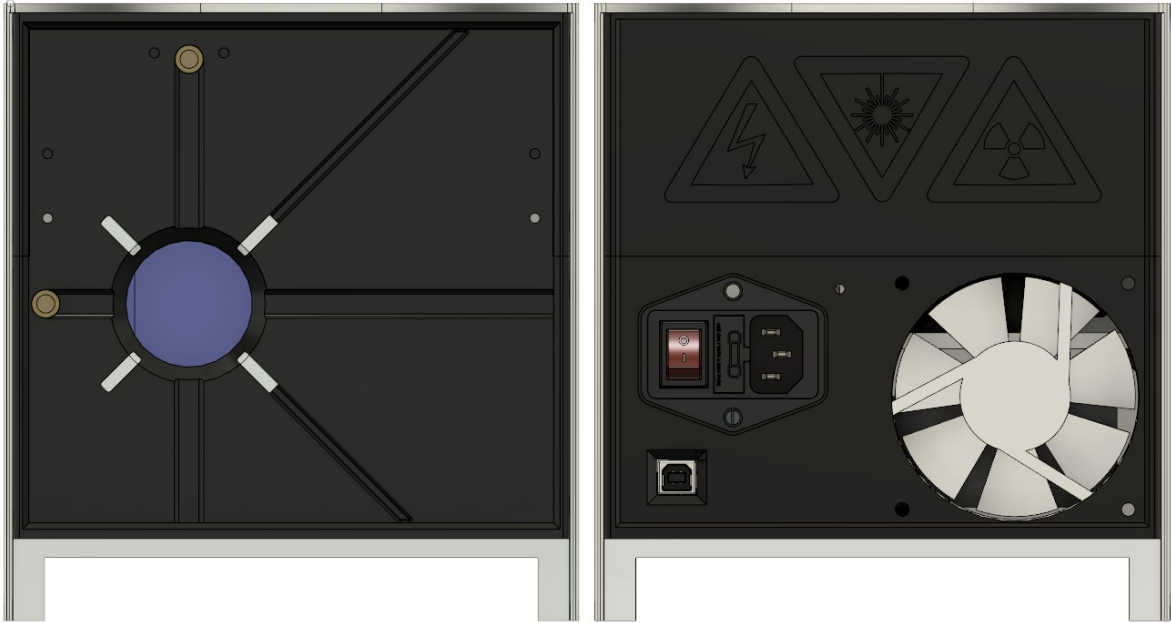Figure 18: First level view.

Figure 19: Second level view.

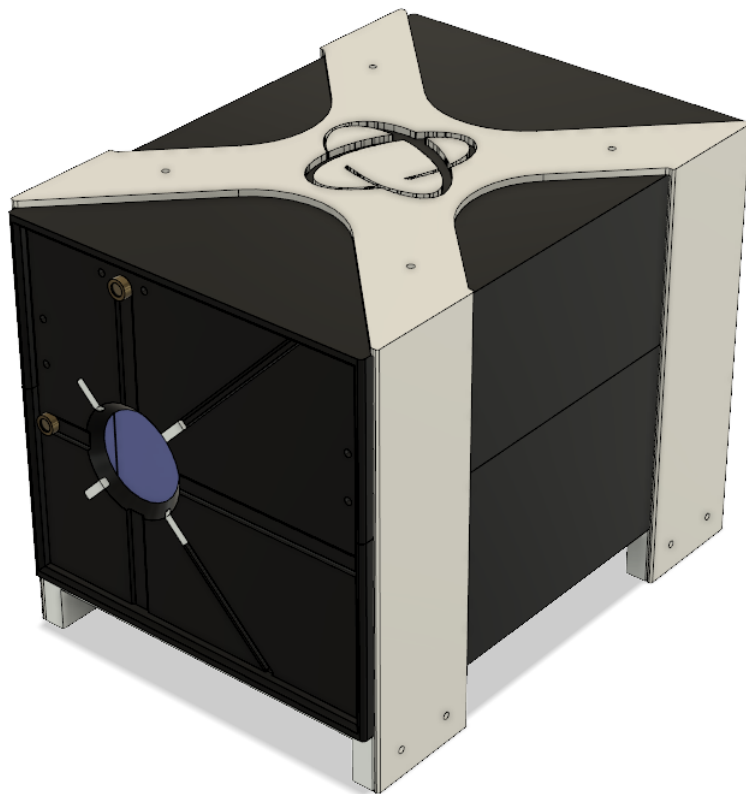Figure 20: Front and back view.

Figure 21: View of the finished design.

Part II

Construction

The design part of the project took the longest time. This was necessary: a good design taking into account all factors and possible incidents during the construction is key. Thanks to a meticulous design, the construction process was fast and fun. However, this does not mean it was easy. We have seen so far how the machine and all its parts will be, but how to make them is a very different thing.

4   The ZVS driver

We saw in section 2.1.3 (after all the failed versions) that the chosen gate driver was the TPS2814P and also the full schematic in figure 10. The circuit was built[10] using a drilled bakelite plate and a small protoboard that contains the TPS2814P, resistances, diodes and 10uF capacitor.
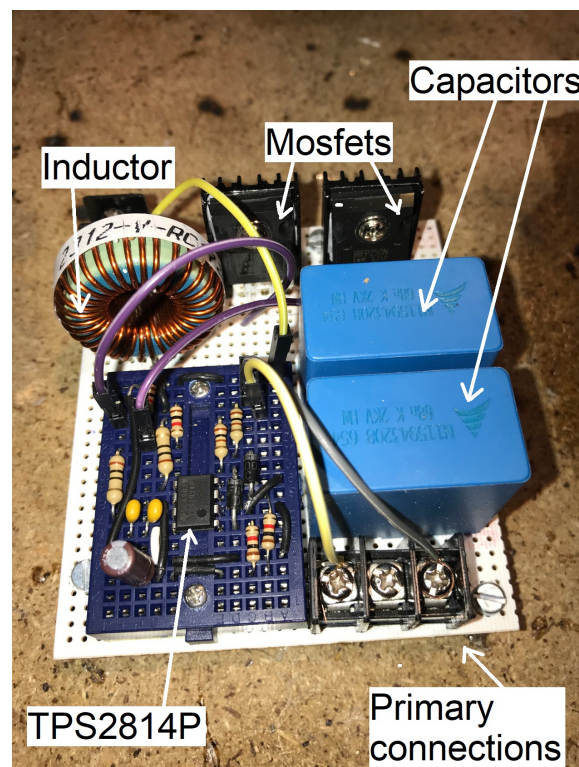

Figure 22: Finished ZVS transformer driver.

This circuit was tested with an ETD59 transformer with 6 turns of primary and 7 of secondary in order to have 126V RMS at the secondary. Three high power resistances were attached to it. A 220Ω resistor was connected in parallel to a 270Ω one and these two in series to another 33Ω resistor for a total load of 154.22Ω. The result of this test was

---

[10]Two small ceramic capacitors were added to the schematic in figure 10 in parallel to the 10uF capacitor to improve transient response. These are the two small yellow capacitors on the protoboard in figure 22.

succesful, the resistances reached 200ºC in 30 seconds. The Mosfets only heated up from 18ºC to 22ºC with a total power of 103W to the load.
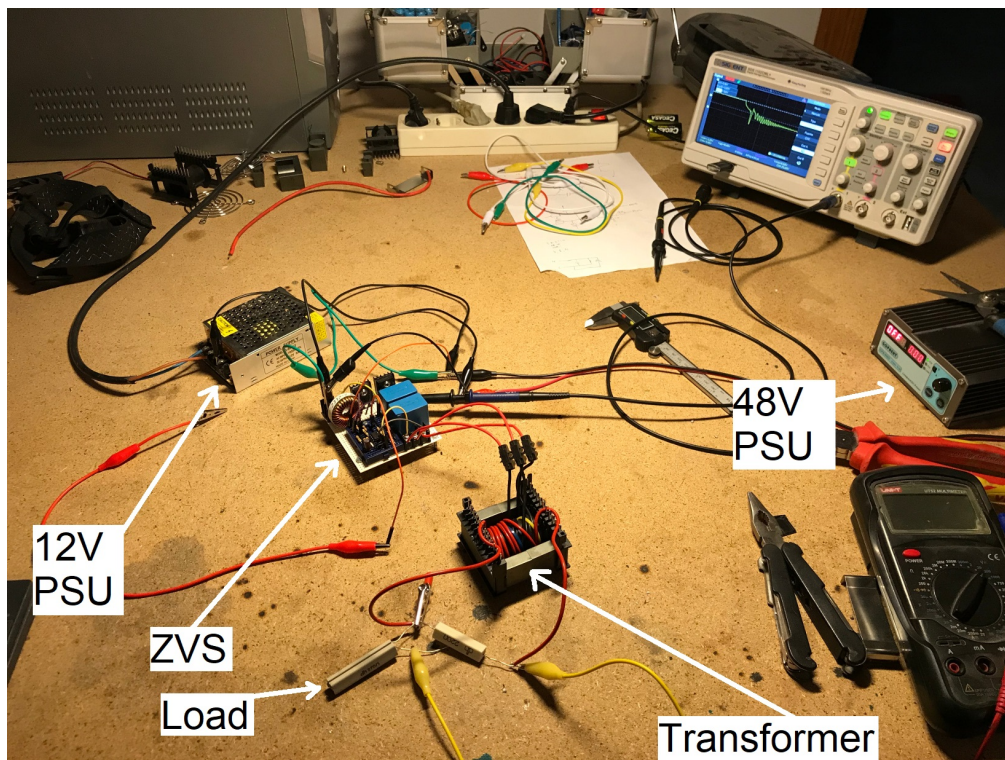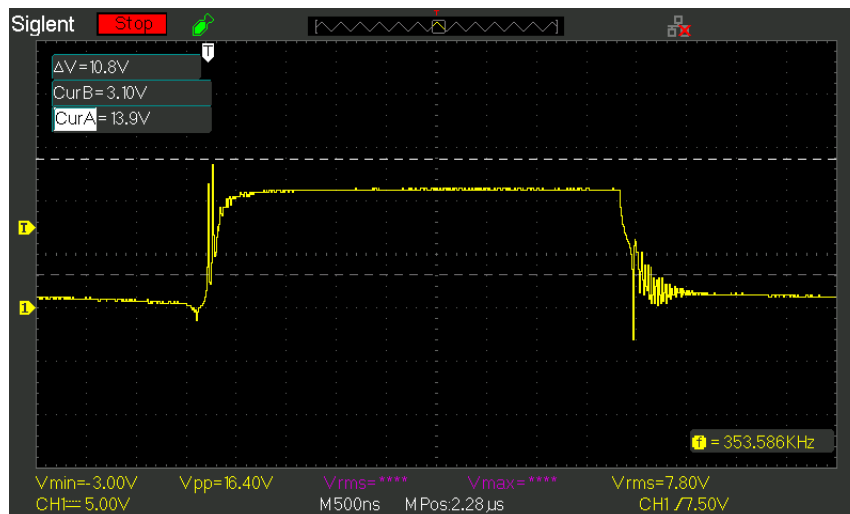

Figure 23: Test bench of the ZVS circuit.

Figure 24: Pulse train waveform at Mosfet gates. We see some notable oscillation at the end, but almost all this noise is very close or below the voltage threshold of the Mosfet[12]. It also lasts for around 500ns only.

In section 2.1.3 it is discussed that the 100Ω resistors next to the diodes were finally placed due to the fact that the noise at the Mosfet gates was lower, figure 25 shows it.

Figure 25: Waveform comparison at Mosfet gates. Up: only diodes. Down: diodes in series with 100Ω resistors.

Noise is present at Mosfet gates and TPS2814P inputs because the high working frequency. Mosfets IRFP250N have little gate charge (123nC [12]), however the gate has to be charged very fast so the circuit can work at high frequency like 116kHz in this project. This means that there is considerable current through the wires at gates. These wires have a parasitic inductance that creates voltage peaks and oscillation shown in figure 24 and 25. Even so, the circuit works, the Mosfets and the gate driver withstand the voltage peaks.
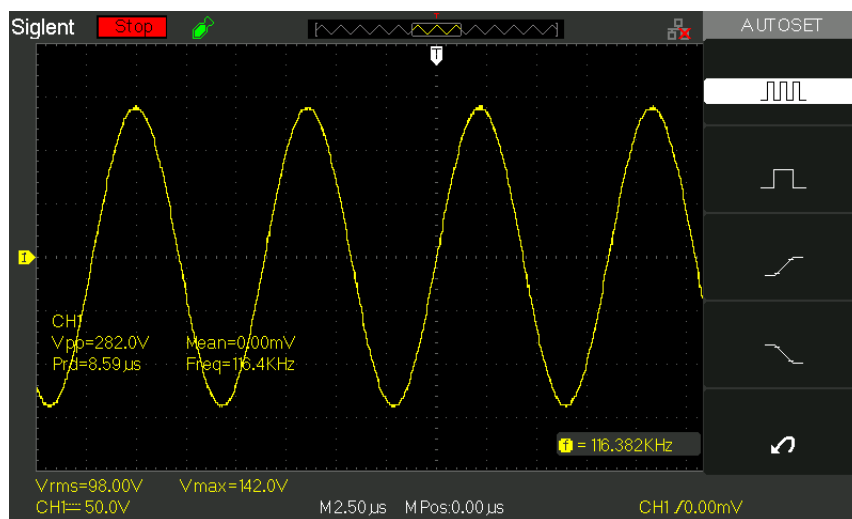

Figure 26: Primary voltage waveform. Despite the noise present at gates and TPS2814P inputs, the primary (and therefore the secondary too) waveforms are clean.

5   High voltage transformer

The inverter circuit is ready to use. The next step is building the 5.5kV ferrite transformer. We saw in section 2.1.2 that the tranformer has these characteristics:

- ETD59 form using N87 ferrite. The core has 1.5mm of air gap.

- The primary is divided in two parts, each one of three turns for a total of six turns. It will run at around 150V and 17A.

- The secondary has 232 turns and will operate at 5.5kV and 24mA RMS.

- The working frequency is around 110kHz.

A manual ETD59 coil winder was designed with Autodesk Fusion 360 and 3D printed. This made the winding process much faster and easier.
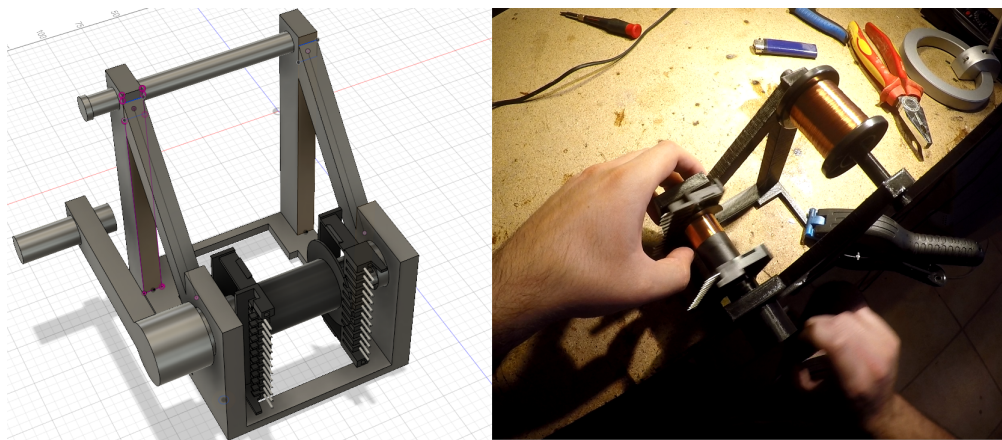

Figure 27: Manual ETD59 winding machine.

The first transformer was made using 0.2mm enamelled wire, however the first layer of turns was complete with some remaining turns to wind, so Epoxy resin was applied to the first layer, then three layers of PTFE tape and the rest of the turns were wound as a second layer above. Then the transformer was tested. It worked for a single second until a bright arc appeared inside the resin. This resin was then partially removed and the transformer was examined with a macro lens that revealed what happened:
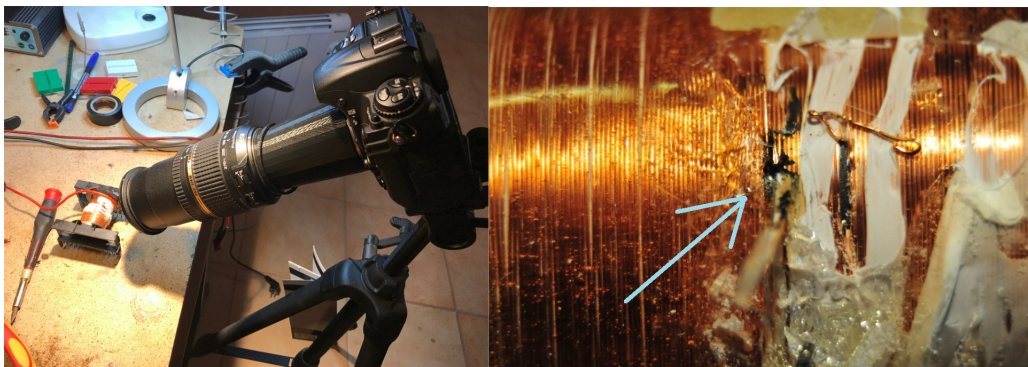

Figure 28: The macro lens revealed that the burnt PTFE tape between the first and second layers of turns was not enough and an arc jumped.

It was necessary to put more isolation between the two layers of windings. A second transformer was then built, this time with three turns of PVC tape, three of PTFE and three of 3M polyester tape.
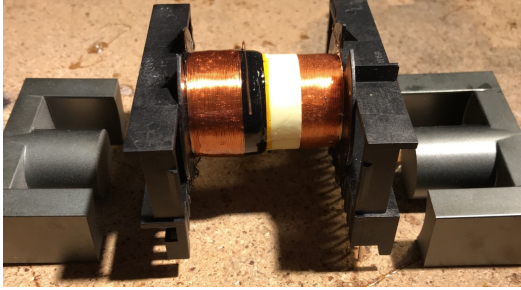

Figure 29: Second attempt of the transformer.

This version managed to work but with poor results. The first and second layers of turns acted as a parasitic capacitor that dropped efficiency of the overall system. It was clear that a third attempt was necessary, but this time using Block 0.15mm wire so all the 232 turns fit in a single layer of turns. This wire can manage the current [14], also taking into account the skin effect [13]:

$$Skin\ Depth\ (\delta) = \sqrt{\frac{2\rho}{2\pi f \mu_r \mu_0}} \qquad (5.1)$$

using copper wire at 110kHz, the skin depth is:

$$\delta = \sqrt{\frac{2 \cdot 1.7 \cdot 10^{-8}\Omega m}{2\pi \cdot 1.1 \cdot 10^5 Hz \cdot \mu_0}} = 0.198mm \qquad (5.2)$$

that is greater (as it should be) than the diameter of the wire (0.15mm). The third transformer was then built with a single layer of turns and several of Epoxy resin. The connections were also welded.
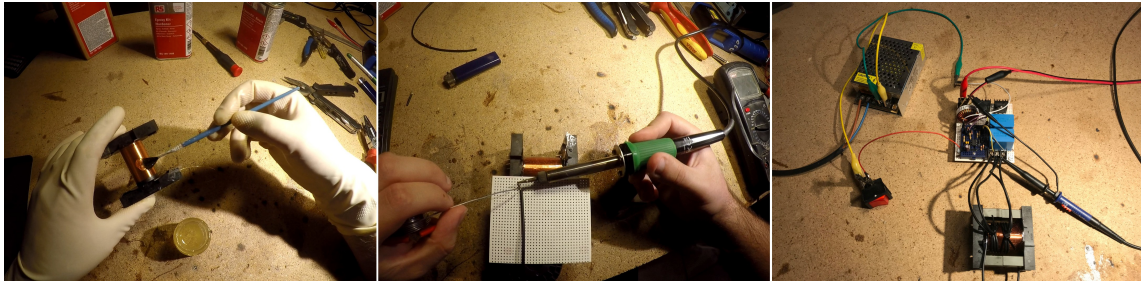

Figure 30: Applying resin, welding connections and testing of the third transformer.

Finally, the third transformer worked as expected. The circuit ZVS+Transformer had losses of around only 14W.

6 The voltage multiplier

As explained in section 2.1.4, the voltage multiplier uses 12 capacitors and 12 diodes in order to multiply the 5.5kV voltage of the transformer output, 12 times, for a voltage of around 65kV. The multiplier was built using FR4 resin board. All joints were welded with caution: it is very important to avoid sharp edges or corona effect can happen. The multiplier also contains the 47kΩ grid resistor for the X-Ray tube. Figure 31 shows the voltage multiplier.

7   The X-Ray head

The X-Ray head is the waterproof box containing the X-Ray tube and multiplier. It is waterproof because it's filled with a liquid insulator, that prevents arcing and also cools down the tube. Liquid paraffin was tested with good results and the head was built and sealed with Epoxy resin.
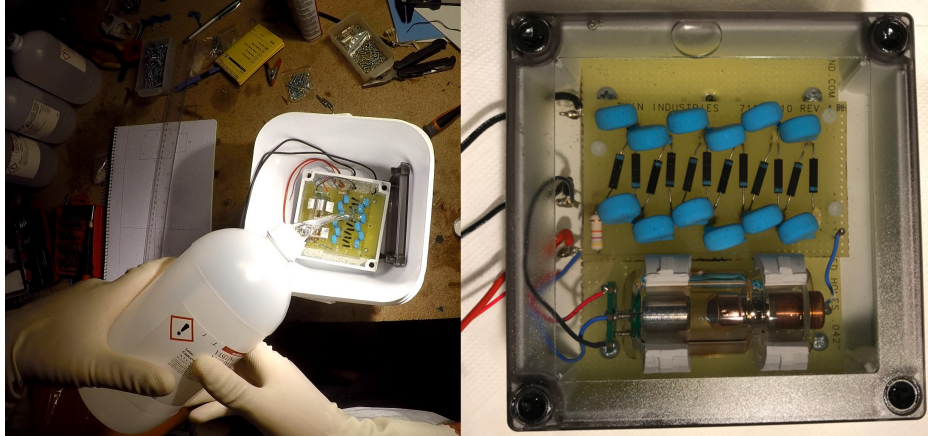

Figure 31: Construction oh the X-Ray head that contains the X-Ray tube and multiplier (blue capacitors and black diodes)

The tube has a read, blue and black wire. The red and blue are the filament, with the blue one grounded. The black wire is the grid and it's connected between the secondary of the transformer and the grid resistor, so the grid will be at lower potential than the filament.

8   Final assembly

All the pieces were ready for the final assembly. This was the fastest part of the project to be finished.
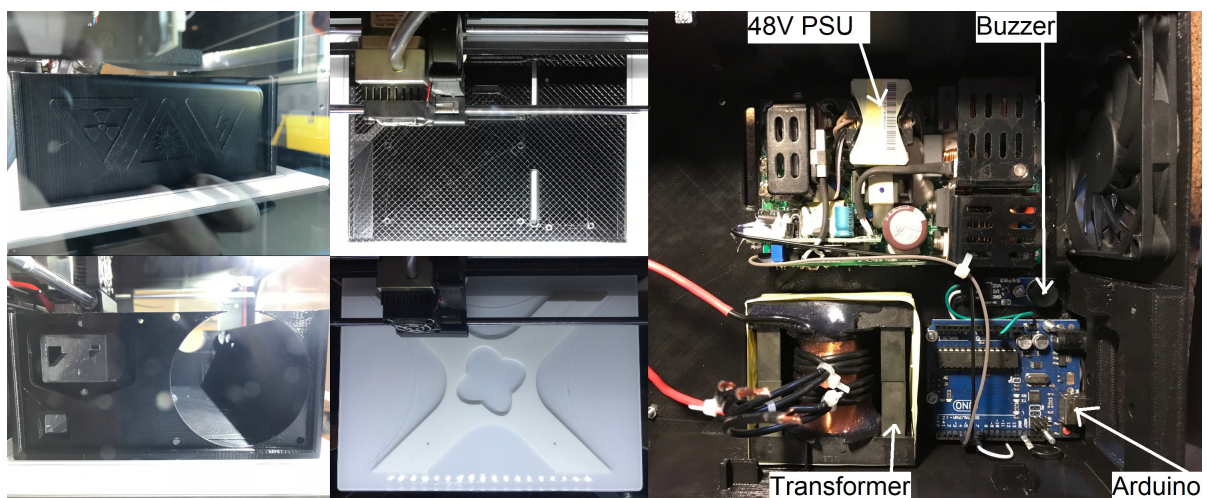

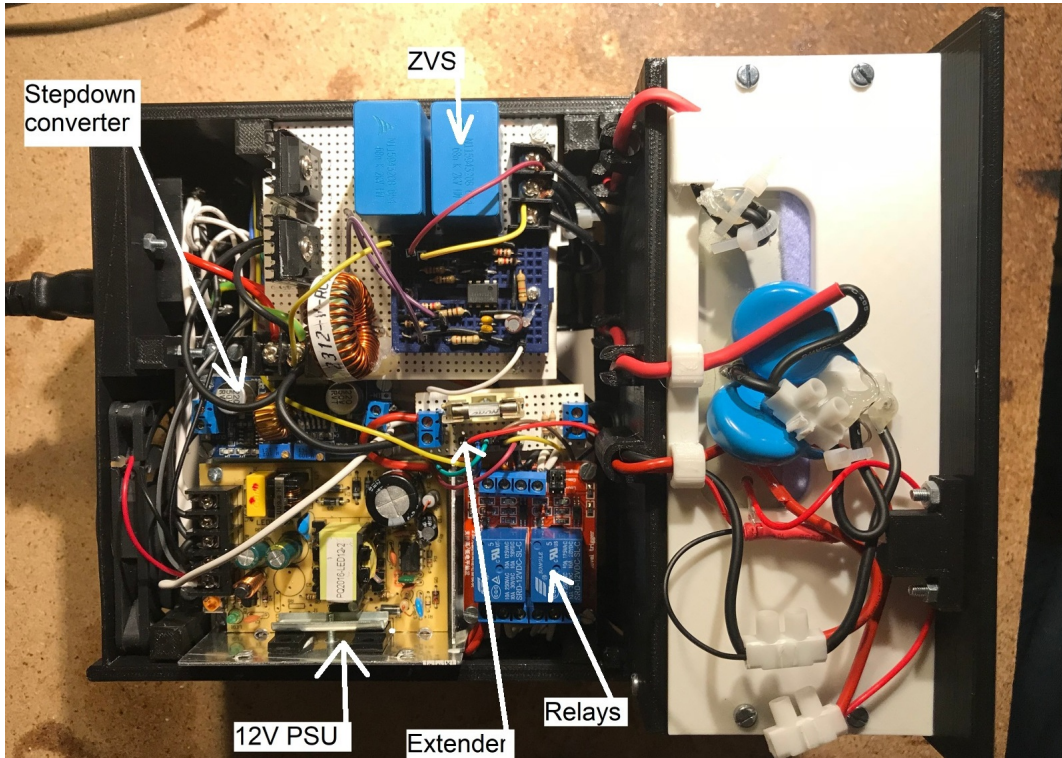Figure 32: Left: printing the housing. Right: first level construction.
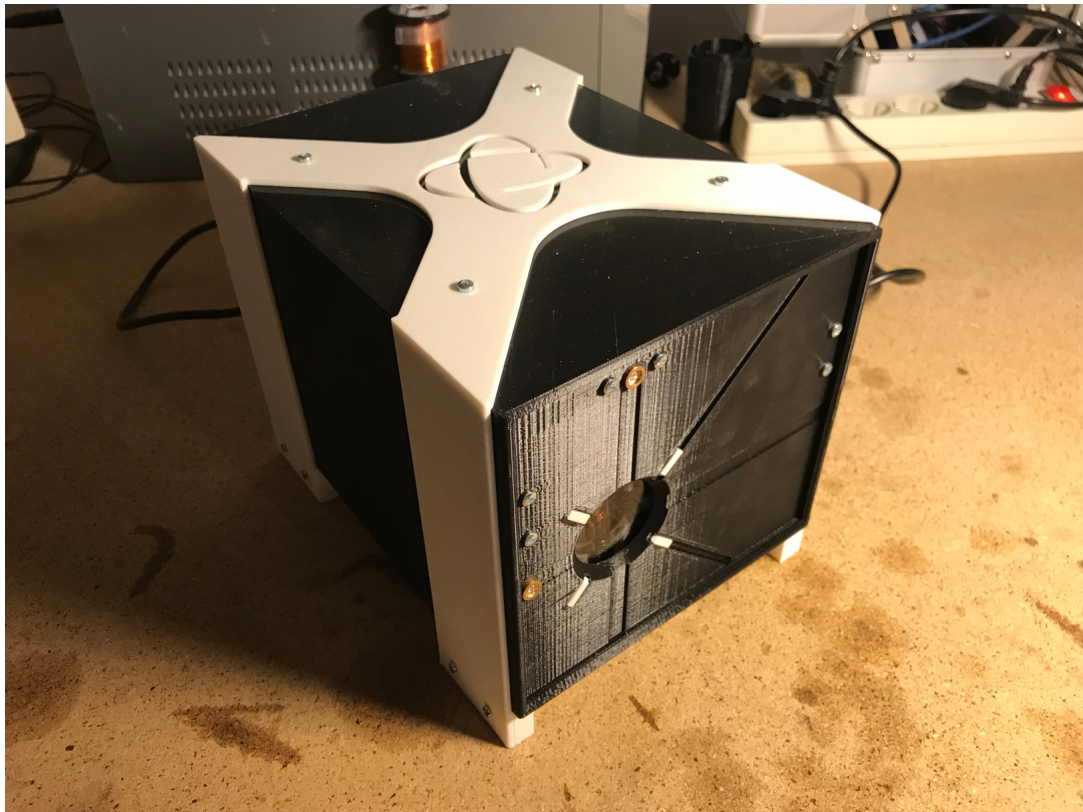
Figure 33: Second level construction.

Figure 34: View of the finished machine.

9   Safety and radiation protection

In this section it is discussed the safety and operativity of the presented machine, also this section is placed after the design and construction on purpose, it's important to first understand how the machine was design and built before explaining why it's safe to operate. So far, we have seen in section 2.2 that Arduino manages the machine and that the machine has lead shielding. We can separate safety measures in electric and radiation protection.

Figure 35: Removing air bubbles from the Epoxy using vacuum.

Regarding electric protection, the machine was designed and built in a way that the risk of fire or shortcircuit is minimized. Due to the high voltage present (around 65kV) it's critical a good insulation.

- The transformer operates at 5.5kV and has a 232 turns secondary, the voltage between turns is 23.7V. The secondary wire was tested to ensure that the enamel could withstand that voltage. A maximum of 60V were applied with no failures.

- As explained in section 7, the X-Ray head is a box filled with liquid paraffin to ensure cooling and electric insulation. The operating voltage (65kV) is not high enough to cause a discharge across the paraffin and the polycarbonate box.

- The X-Ray tube operates with its cathode grounded. Grounding is very important because we don't have floating voltages and we know exactly the parts of the machine that are at high potentials.

- The Epoxy resin applied to the transformer to fix its windings and to the X-Ray head to seal it was previously put in a vacuum chamber (figure 35) to remove air bubbles that can affect the dielectric strenght.

- The plastic housing and remote control of the machine ensures that the operator is not at risk of being electrocuted.

Radiation protection is considered with the following key points:

- The X-Ray head has 1mm of lead shielding all around, except for the front, were X-Rays are emitted.

- The machine is designed to be used only with small objects and it's placed in a basement.

- The machine is controlled remotely via remote desktop application to the laptop it's connected to. The operator is not present in the room or near it.

- The Geiger counter reads no counts except for background radiation where the operator is present at the moment of activation of the machine.

- The power is not as high as a commercial unit[11], but it's powerful enough to create radiographs using very short exposures[12].

---

[11]The total power of the machine is 80W. Power of commercial dental machines can be found above 400W.

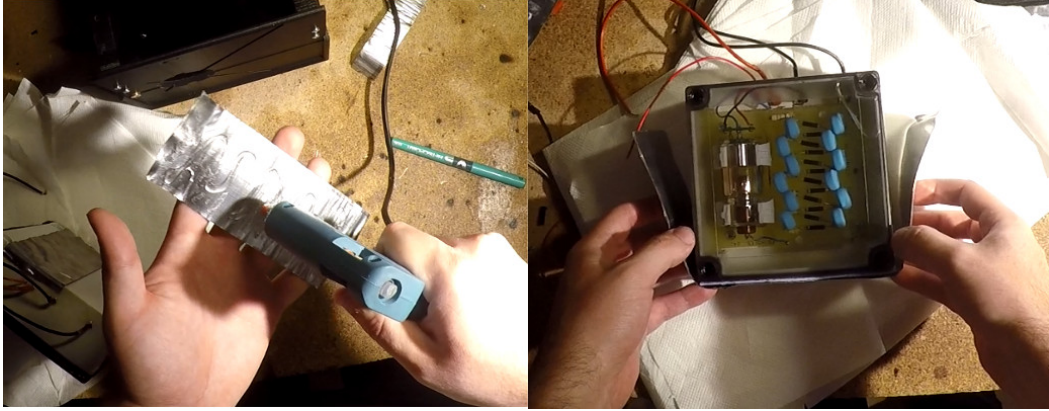[12]Most of the radiographs were taken with just one second of exposure.

Figure 36: The lead sheets are glued to the X-Ray head.

X-Rays follow an exponential attenuation law using two coefficients, the linear attenuation coefficient μ and the energy absorption coefficient μ_{en}. The difference is that μ counts the photons that don't interact with the material and μ_{en} considers scattering that make some of the incident photons cross the material but with less energy [1]. These coefficients are used with the following formulas[13]:

$$N = N_0 e^{-\mu x} \tag{9.1}$$

$$E = E_0 e^{-\mu_{en} x} \tag{9.2}$$

Due to the Bremsstrahlung effect, X-Rays will be emitted in a wide range of energies with a maximum in keV of the corresponding voltage in kV applied to the tube. The working voltage is around 65kV, so the maximum energy of an X-Ray photon will be 65keV. The next step is gathering coefficient data from NIST [15]. The coefficients for 65keV are not tabulated but NISTX [16] utility is used to interpolate. For 65keV, the coefficients are $\mu = 46.51 cm^{-1}$ and $\mu_{en} = 37.98 cm^{-1}$. With these values we can use ecuations 9.1 and 9.2 to find the attenuation and absorption values:

$$\% \, of \, attenuated \, photons = 100(1 - \frac{N}{N_0}) = 100(1 - e^{-46.51 \cdot 0.1}) = 99.04\% \tag{9.3}$$

$$\% \, of \, energy \, absorbed = 100(1 - \frac{E}{E_0}) = 100(1 - e^{-37.98 \cdot 0.1}) = 97.75\% \tag{9.4}$$

We see that almost all the X-Rays are removed by the shielding. However, the most important safety measure is not the shield but the remote control. Although the shield is effective, the operator would have to operate the machine next to it if no remote control is available, but with this feature, the operator can control the machine anywhere in the world. In this project, the remote control is considered the machine most important key feature. It guarantees total safety for the operator.

---

[13]N is the photons that cross the material without interacting, N_0 is the incident number of photons, E_0 is the incident energy, E is the measured energy after the material and x is the material width.

Part III

Results

10   Single color 2D radiography

In this section it is presented the results of regular radiography with some objects.

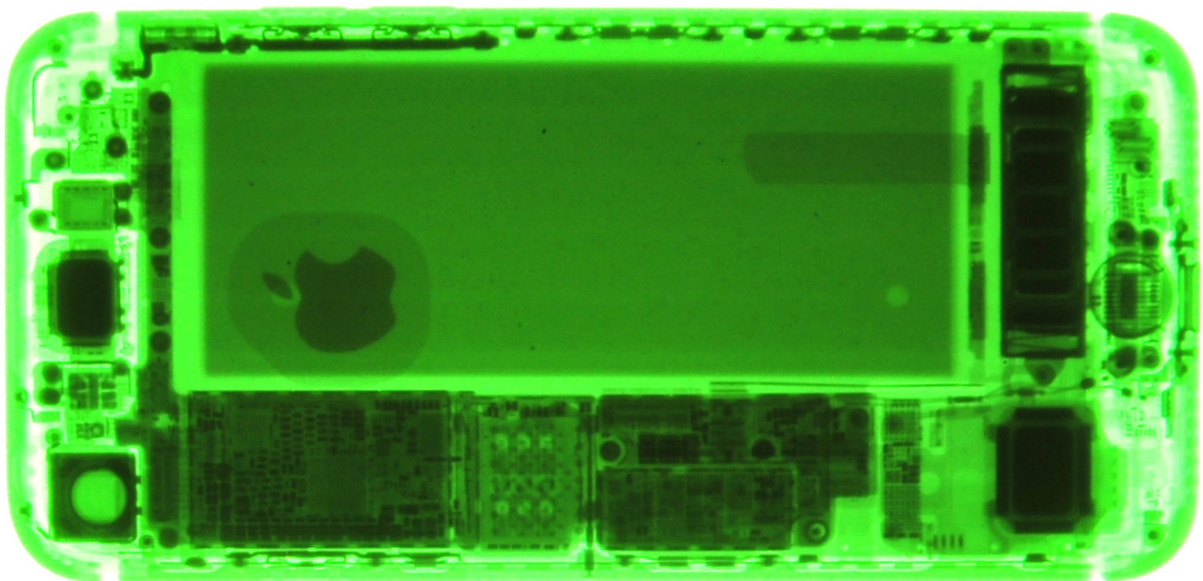Figure 37: Left: videocamera. Right: Geiger counter.

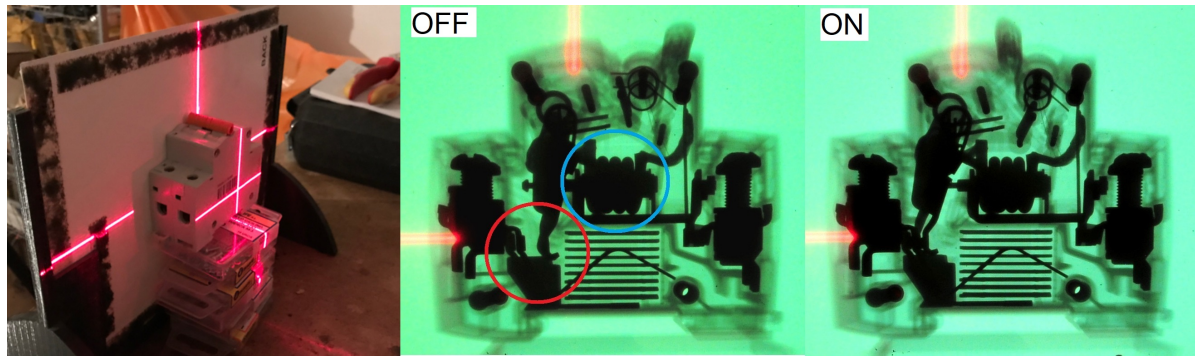Figure 38: iPhone 7, the cover image of this paper.

Figure 39: General switch. The red circle shows the contact, the blue one shows the inductor that triggers the switch if the current is too high.

11 Pseudocolor 2D radiography

As seen in section 10, the radiographs taken are green because the scintillation screen used to reveal the X-Rays glows green. This gives us a single color image, but there are algorithms that can color the image taken, for example, assigning red to most opaque objects and blue to most transparent to radiation. In this section it's presented the results of applying the algorithm explained in appendix B. All pictures are divided in four sections, the upper left image is the original and the rest are pseudocolored using different thresholds[14] increasing from left to right.
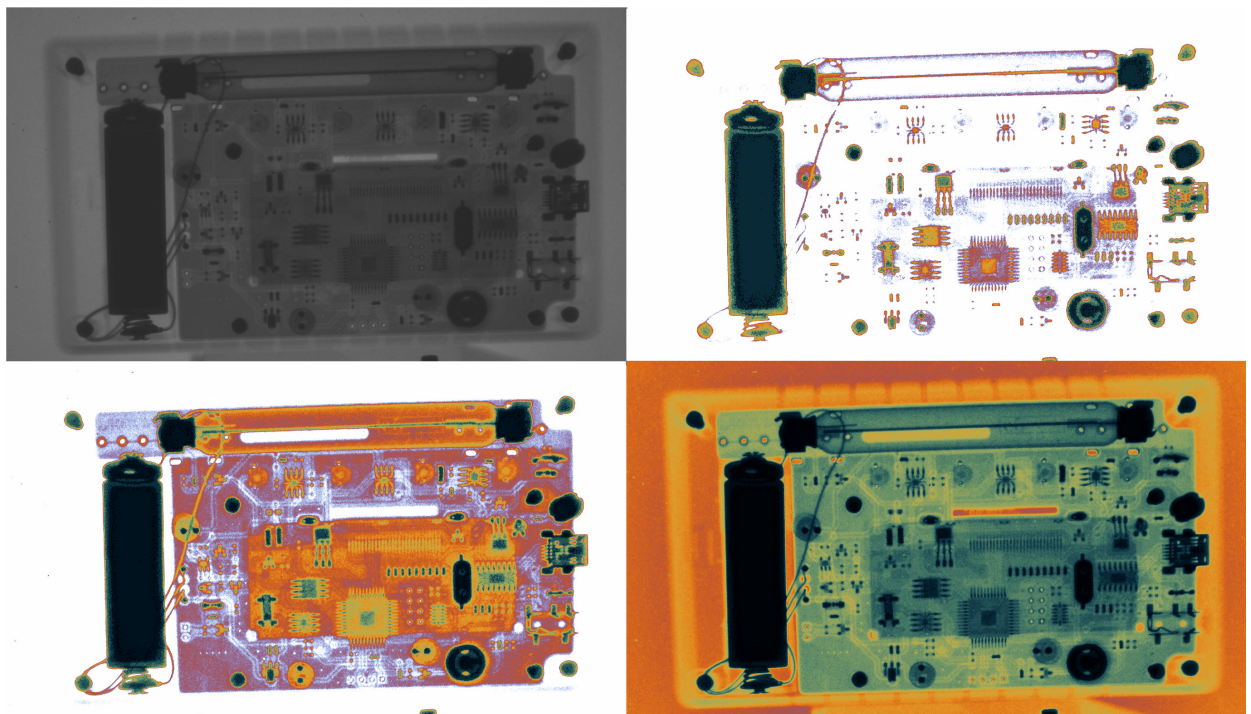

Figure 40: Geiger counter.

---

[14]More about this threshold is explained in appendix B. In brief, it has the effect of highlighting color of opaque parts to X-Rays and attenuating the most transparent while recoloring the entire image.
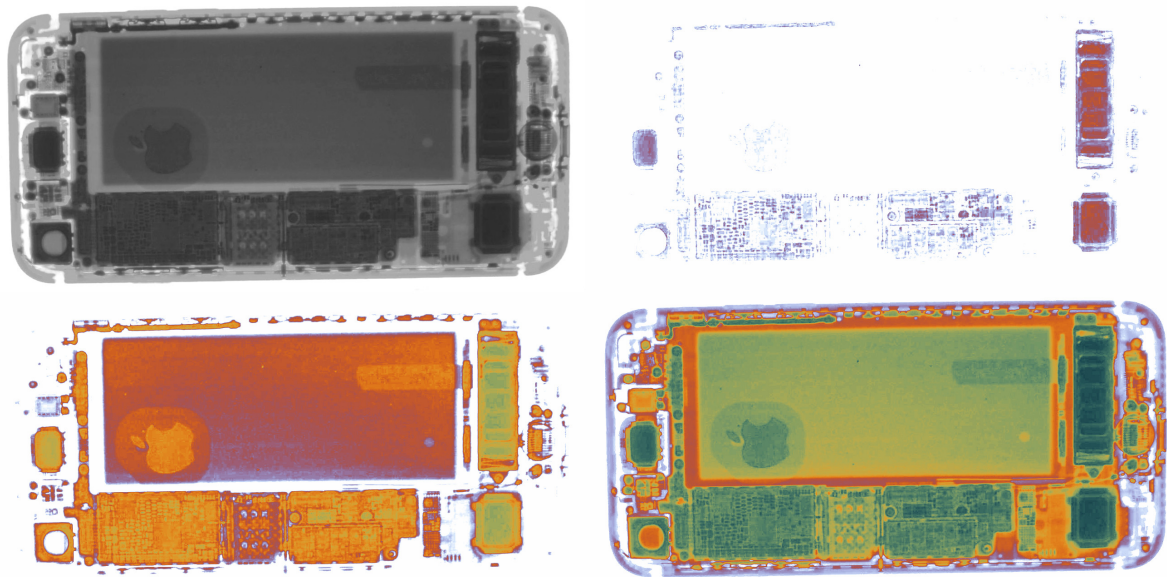
Figure 41: iPhone 7. At low threshold (upper right image) only the three most opaque parts to X-Rays are noticeable, the front and bottom speakers and the Taptic Engine.

Figure 42: Hot glue gun. At low threshold (upper right image) only metal parts (and some high density plastic) are shown.

We see that a RGB colored image can be created from a single color radiography using algorithms. This technology is used, for example, in airport security, where it's needed to differentiate objects as fast as possible. This is done assigning different colors to different opacities.

12 Tomographic 3D radiography

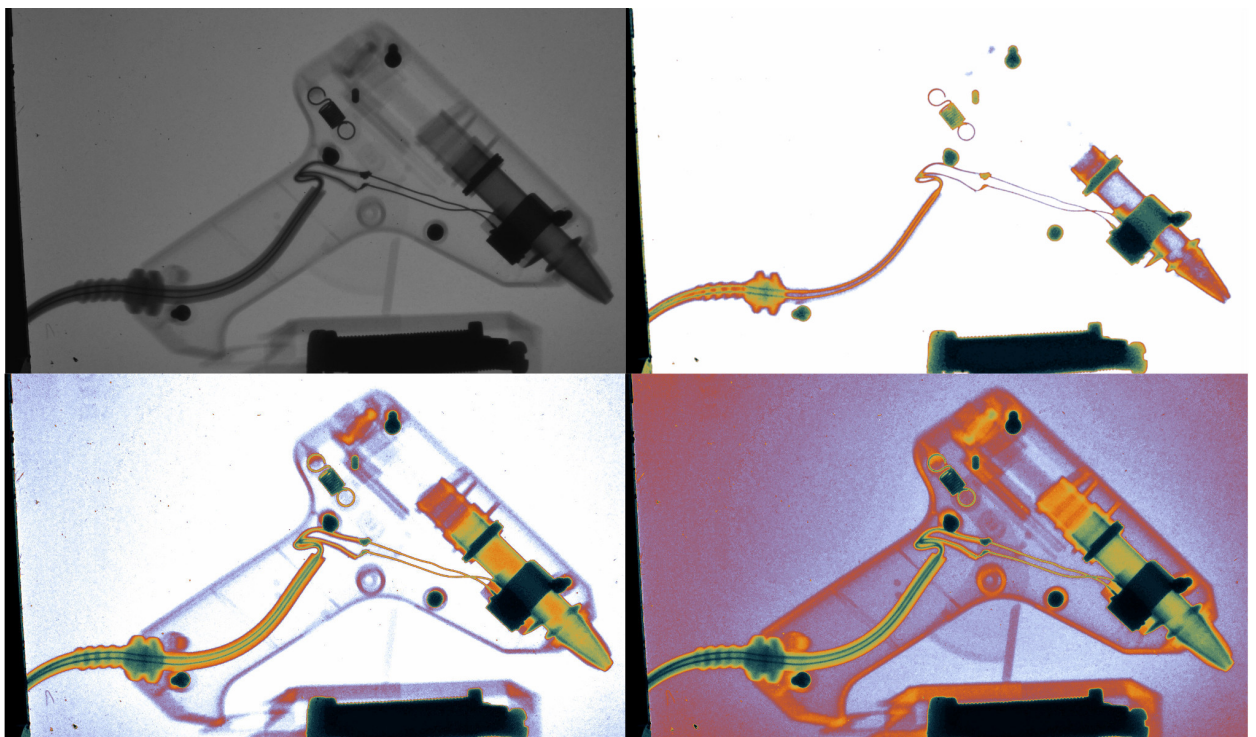Tomographic reconstruction is the process of recreating the front view image of a slice of the object. In appendix A it's explained the algorithm used to perform these 3D reconstructions. Unlike regular radiography, Computerized Tomography (CT) scans needs radiographs from different angles around the object to study. In order to gather this data, a videocamera was used. The object to study is placed on a motor that rotates it and the machine is configured to X-Ray for three seconds, so the object is recorded spinning through X-Rays. Then the algorithm is applied and the reconstructed data (in the form of cloud of points) is analized using a point cloud viewer[15]. The machine and the algorithm were tested to prove that they can retrieve information such as the gas content of a lighter with an opaque sticker and the internal components of an LED panel lamp.
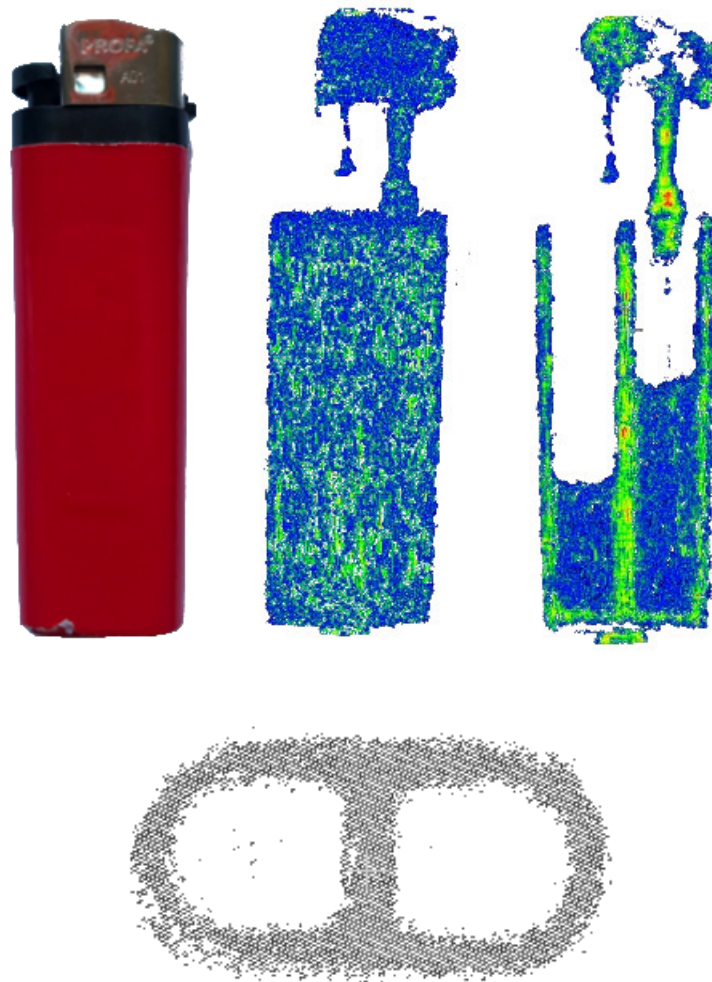

Figure 43: CT reconstruction of a lighter. In the upper image, the walls are removed via software so we can retrieve data about the content in gas. The lower image shows a slice.

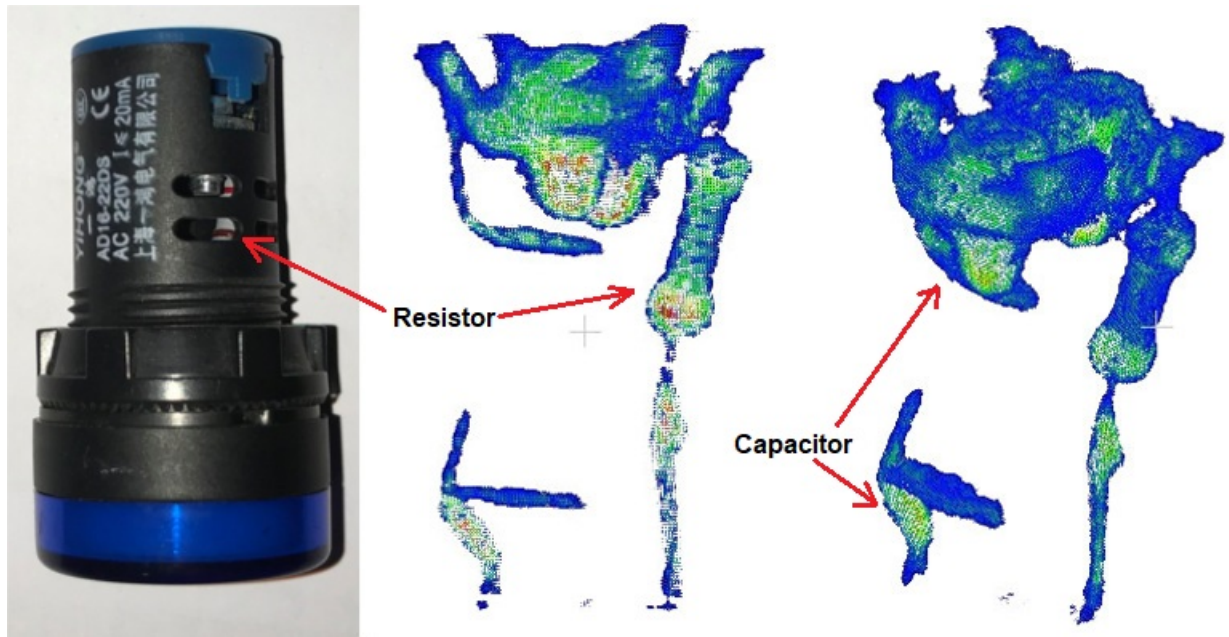[15]Cloud Compare was used to view the data.

Figure 44: CT scan of an LED panel lamp. We can see two screws on the top, a resistor and a capacitor. The capacitor itself is very transparent to X-Rays so we only see its pins.
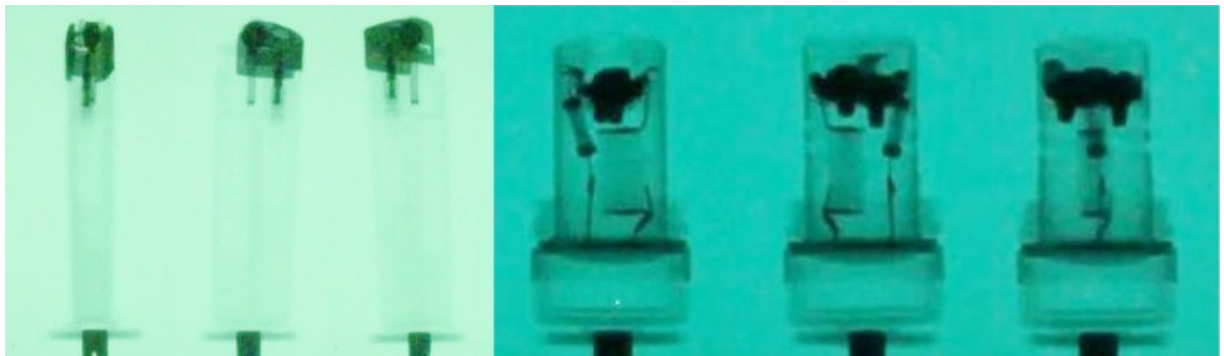
Figure 45: Example of the data recorded and used to make the 3D reconstruction for the lighter and the LED panel lamp.

We can see that the reconstructed 3D objects have noise. This is mainly because we have very few images available from different angles. The camera records at 25fps, if the object rotates a full turn in approximately three seconds[16], then we only have around 75 images. More images make cleaner reconstructions[17].

Despite the noise, the reconstructions can provide useful information about the inside of small obects. We were able to retrieve the gas level of the lighter and determine that the lamp has a resistor and a capacitor.

---

[16]The motor used to rotate the object has a fixed speed.

[17]The algorithm developed in this project uses linear interpolation between images, so we can increase the number of images available. This has the effect of more blurry results but almost free of noise [19].

13   Conclusion

In this paper, we have seen that a reliable X-Ray machine could be designed, built and tested. The construction of the high voltage source for the X-Ray tube required an innovation of the original ZVS Mazzilli driver found on the internet. The addition of a Mosfet driver makes this circuit capable of working at more frequency, also improving switching speed and efficiency. A high voltage transformer was built and tested with succesful results.

In this project, the experiments with the pieces of the machine were key to ensure safety. The Epoxy resin and liquid paraffin isolate the high voltage parts of the machine, ensuring electric protection. On the other hand, the lead shielding and the remote control feature ensures radiation protection for the operator, that can manage the machine as far from it as desired.

The results prove the success of this project. Regular 2D radiography images are sharp and provide useful information about the inside of the objects, the machine can be used for diagnosis of small mechanical objects like the general switch. Regular radiography images can also be colored using pseudocolor algorithms. The one developed in this project has proven to make easier the detection of metal parts without saturating color. Finally the machine was used to perform CT scans of a lighter and an LED panel lamp, proving that it is also capable of tomographic reconstructions using an algorithm on the data gathered.

A   The CT reconstruction algorithm

In this appendix it's explained the algorithm used to perform the 3D reconstructions shown in section 12. There are several algorithms used to make tomographic radiography, the one used in this project is an implementation of the Filtered Back Projection, an algorithm that uses the inverse Radon transform. To understand the algorithm, first consider a planar object that looks like the left image in figure 46:
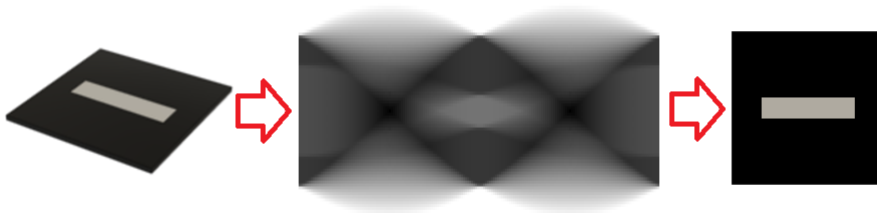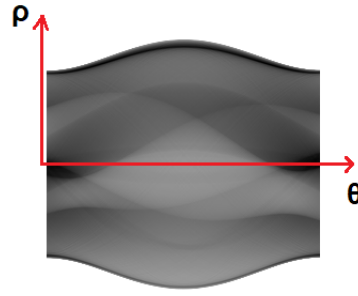

Figure 46: Reconstruction process [17].

An X-Ray machine rotates around the object, making N radiographs from N different angles. Consider that the radiographs taken are just a row of pixels since the object is planar. All these rows of pixels are transposed to columns and put together. The result image is the center one in figure 46 and it's called sinogram.

The sinogram contains all the information about how a slice of the object looks from N different angles. Each column of pixels in the sinogram is just the X-Ray image of the slice at a given angle. The first column is angle 0 and the last is usually angle 360.

Figure 47: Example of sinogram and its coordinates. The pixel at (θ, ρ) is the pixel of the object at ρ distance from axis and angle θ.

The algorithm takes the sinogram and reconstructs the view of the slice, applying the inverse Radon transform (Back Projection algorithm) [17][18]:

$$f(x,y) = \int_0^{2\pi} f'(xcos(\theta) + ysin(\theta), \theta)d\theta \tag{A.1}$$

where f is the reconstructed image of the slice and f' is the sinogram. The discrete version of this integral with a total of N radiographs is:

$$f(x,y) = \Delta\theta \sum_{n=0}^{N-1} f'(xcos(\theta_n) + ysin(\theta_n), \theta_n) \tag{A.2}$$

However, if we apply equation A.2 to the sinogram, the result is blurry. This is because we have a finite number of X-Ray images at different angles. To solve this, the sinogram is filtered before using equation A.2. A forward Fourier transform is applied to each column of the sinogram, then the values of each column are multiplied by a high pass filter [18] and an inverse Fourier transform gives us the same sinogram but filtered. When using equation A.2 on a filtered sinogram, the result is sharper. Figure 48 shows the difference when a filtered sinogram is used[18].
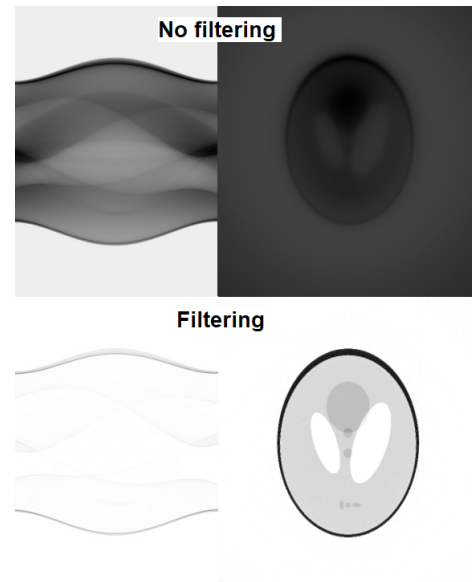

Figure 48: Back projection with a filtered and unfiltered sinogram.

When the sinogram is filtered before applying equation A.2, the algorithm is called Filtered Back Projection (FBP).

---

[18]The reconstructed image in figure 48 is called "Shepp-Logan Phantom" [27] and it's used for testing reconstruction algorithms.

So far we now understand how the sinogram of a slice of an object is made (the X-Ray machine rotates around the object[19]) and how the algorithm is used to create the axial view of that slice. The next step is extending that to a full object, resulting in a set of slices. Each one will have its own sinogram, and applying the FBP algorithm to all sinograms will result in a 3D reconstruction like those shown in section 12.
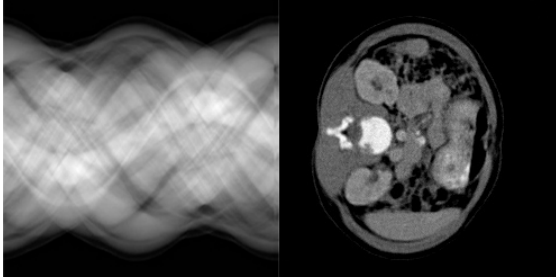

Figure 49: Example of the developed program in action [20].

The complete C++ implementation of the Filtered Back Projection developed in this project can be found on GitHub [19] in the form of library ready to be used. OpenCV is the image manipulation software used, it also allows the Fourier transform for filtering the sinogram. The filter used is the following:

$$g(\omega) = \frac{1}{2\pi} \left| \sin(\frac{\omega \pi}{\omega_{max}}) \right| \qquad (A.3)$$

The software developed has been designed to reconstruct single sinograms[20] as well as 3D objects directly using the data recorded by the videcamera.
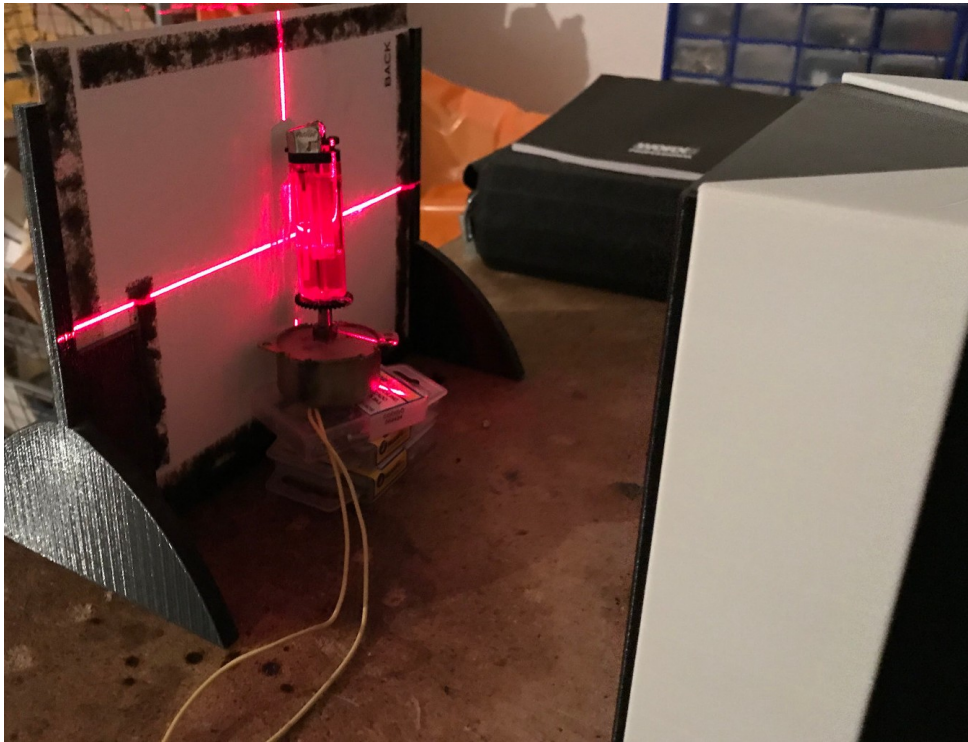

Figure 50: Example of the experimental method for the 3D reconstruction of the lighter. It's shown the motor, the machine and the scintillation screen..

---

[19] In this project, it is the object that rotates. In medical CT scanners, the machine rotates around the body.

[20] The program was tested with some sinograms found on the internet, like the one in figure 49.

B   The pseudocolor algorithm

As shown in section 11, the radiographs taken are single color because scintillation screens glow to X-Rays in just one color, usually green, but they can be colored using pseudocolor algorithms. This consists of just a $\mathbb{R} \rightarrow \mathbb{R}^3$ function that takes the brightness of every pixel of the input image (in the integer range of 0 to 255 for 8bit images) and gives a 3-tuple [R,G,B] that is the pseudocolor of the pixel.

The algorithm developed in this project has been called Helix Pseudocolor Algorithm, also available on GitHub [21]. It considers a three dimensional space with a cartesian coordinate system RGB, with values for each axis from 0 to 255. It's clear that a line connecting (0,0,0) to (255,255,255) contains all grayscale values. The only thing to do next is creating a curve inside that space, that can be any. It was chosen to make a curve that connects the origin to (255,255,255), so if the input brightness is zero, the output color is (R,G,B)=(0,0,0) (black), and if its 255, the ouput is (255,255,255) (white).

The curve designed has a helix shape and starts this way:

1. First we consider a circunference with this equation:

$$B = \rho cos(\phi) \quad R = \rho sin(\phi) \tag{B.1}$$

2. We add a G dependence and parametrize ϕ with t (brightness) so that when t=255 (maximum brightness) a full turn is completed and $G = 255\sqrt{3}$.

$$B = \rho cos\left(\frac{2\pi}{255}t\right) \quad R = \rho sin\left(\frac{2\pi}{255}t\right) \quad G = t\sqrt{3} \tag{B.2}$$

3. We now have the parametric equation of an helix. In order to make this curve start and end on G axis, we change ρ by $\rho_{sat}sin\left(\frac{\pi}{255}t\right)$, where ρ_{sat} becomes a saturation parameter that will allow us to choose the color saturation.

$$B = \rho_{sat}sin\left(\frac{\pi}{255}t\right)cos\left(\frac{2\pi}{255}t\right) \quad R = \rho_{sat}sin\left(\frac{\pi}{255}t\right)sin\left(\frac{2\pi}{255}t\right) \quad G = t\sqrt{3} \tag{B.3}$$

4. The next step is rotating this curve first 54.73º around B axis (R_B) and then 45º around G (R_G). These angles are chosen so the curve now starts in (0,0,0) and ends in (255,255,255) as we wanted. RGB is the modified helix from equation B.3 and R'G'B' is the rotated curve.

$$\begin{pmatrix} R' \\ B' \\ G' \end{pmatrix} = R_G R_B \begin{pmatrix} R \\ B \\ G \end{pmatrix} = \begin{pmatrix} cos(45º) & -sin(45º) & 0 \\ sin(45º) & cos(45º) & 0 \\ 0 & 0 & 1 \end{pmatrix} \cdot$$

$$\cdot \begin{pmatrix} cos(54.73º) & 0 & sin(54.73º) \\ 0 & 1 & 0 \\ -sin(54.73º) & 0 & cos(54.73º) \end{pmatrix} \begin{pmatrix} R \\ B \\ G \end{pmatrix} \tag{B.4}$$

5. Substituting RGB in equation B.4 by their values given in equation B.3 and applying matrices, these are the final equations:

$$B'(t, \rho_{sat}) = \rho_{sat}sin\left(\frac{\pi t}{255}\right)\left[0.707cos\left(\frac{2\pi t}{255}\right) + 0.408sin\left(\frac{2\pi t}{255}\right)\right] + 0.577t\sqrt{3} \quad \text{(B.5)}$$

$$R'(t, \rho_{sat}) = \rho_{sat}sin\left(\frac{\pi t}{255}\right)\left[-0.707cos\left(\frac{2\pi t}{255}\right) + 0.408sin\left(\frac{2\pi t}{255}\right)\right] + 0.577t\sqrt{3} \quad \text{(B.6)}$$

$$G'(t, \rho_{sat}) = 0.577t\sqrt{3} + 0.816\rho_{sat}sin\left(\frac{\pi t}{255}\right)sin\left(\frac{2\pi t}{255}\right) \quad \text{(B.7)}$$

Equations B.5, B.6 and B.7 give the pseudocolored R'G'B' values for a pixel with brightness t. The parameter ρ_{sat} is chosen depending on the desired saturation and it must not exceed a value that makes the curve cross the 255x255x255 space. The value 140 is used in this project.
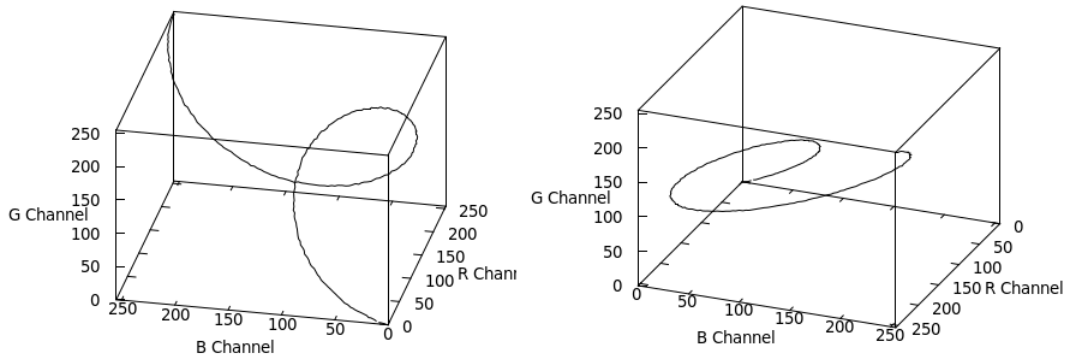

Figure 51: Designed curve in the RGB space.

In section 11 it's mentioned a threshold, that is applied before equations B.5, B.6 and B.7: the brightness of all pixels get a new value given by $B = B_0\frac{255}{Th}$, where B and B_0 are the new and initial brightness respectively and Th is the threshold. If the new brightness B is greater than 255, it's assigned 255. Applying this threshold removes the background, leaving the object to study alone. It also attenuates the most transparent parts to X-Rays, leaving the most opaque zones highly colored, as shown in figure 52.
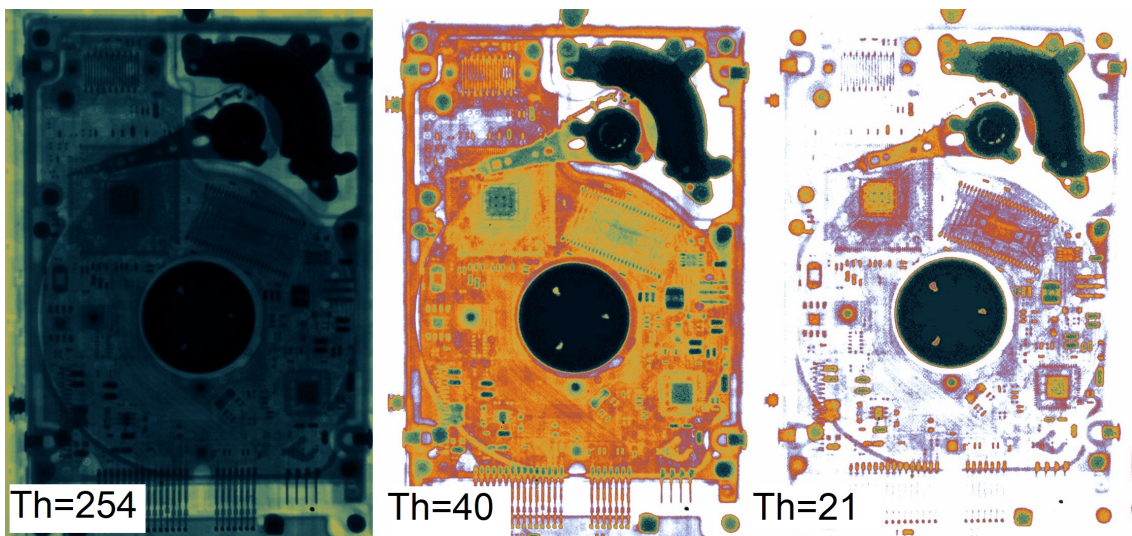

Figure 52: Hard disk drive pseudocolored using three different thresholds. At low threshold, only thick metal parts are highlighted in dark green, so the algorithm works.

C The ZVS simulation program

The last C++ program developed in this project consists of a numerical model for the Mazzilli ZVS. This model only attempts to reproduce the same values given by OrCAD for the resonant mesh and secondary voltage, that are the most important values.
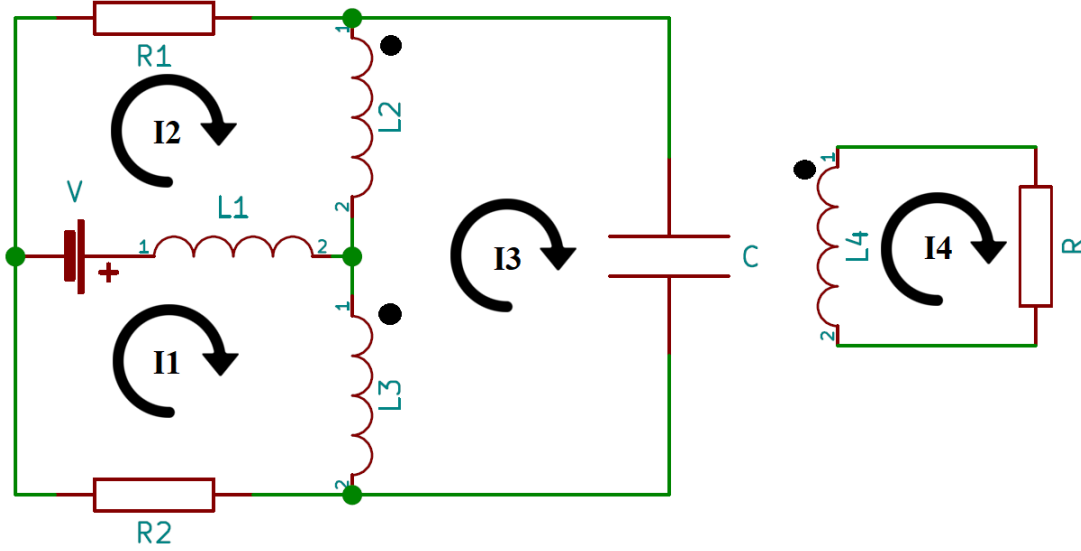

Figure 53: ZVS Mazzilli driver numerical model of the original circuit in figure 3.

The model works this way:

- Resistors R1 and R2 simulate the two Mosfets. Their values vary in time like a pulse train of frequency that matches the resonant of the primary (L2 and L3) and capacitor C, with values from 0Ω to a considerably high resistance (it's used $100M\Omega$). This way, these resistances act like the Mosfets. Resistor R is the load.

- Inductors L2, L3 (these two are the primary) and L4 (secondary) are coupled. Inductor L1 is characteristic of any Mazzilli ZVS and it's only used to stabilize current. Indutors L2 and L3 have the same value (L2 from now on).

- M_{23} is the mutual inductance of L2 and L3, but since they have the same value, $M_{23} = L2$. M_{24} is the mutual inductance of L2 (or L3) and L4.

The mesh currents method is used to solve this circuit:

$$Mesh\,1: \ V = L_1(I'_1 - I'_2) + L_2(I'_1 - I'_3) - M_{23}(I'_3 - I'_2) - M_{24}I'_4 + R_2I_1 \quad (C.1)$$

$$Mesh\,2: \ -V = L_1(I'_2 - I'_1) + L_2(I'_2 - I'_3) - M_{23}(I'_3 - I'_1) - M_{24}I'_4 + R_1I_2 \quad (C.2)$$

$$Mesh\,3: \ 0 = \int_0^t \frac{I_3}{C}dt + L_2(I'_3 - I'_1) + M_{23}(2I'_3 - I'_2 - I'_1) + L_2(I'_3 - I'_2) + 2M_{24}I'_4 \quad (C.3)$$

$$Mesh\,4: \ 0 = RI_4 + L_4I'_4 + M_{24}(I'_3 - I'_1) + M_{24}(I'_3 - I'_2) \quad (C.4)$$

Solving for mesh currents:

$$I_1' = \frac{V + L_1 I_2' - L_2 I_2' + 2L_2 I_3' + M_{24} I_4' - R_2 I_1}{L_1 + L_2} \tag{C.5}$$

$$I_2' = \frac{-\left(V + R_1 I_2 + L_2\left(I_1' - 2I_3'\right) - L_1 I_1' - M_{24} I_4'\right)}{L_1 + L_2} \tag{C.6}$$

$$I_3' = \frac{-\int_0^t \frac{I_3}{C} dt - 2L_2\left(I_1' + I_2'\right) + 2M_{24} I_4'}{4L_2} \tag{C.7}$$

$$I_4' = \frac{-\left(R I_4 + M_{24}\left(2I_3' - I_1' - I_2'\right)\right)}{L_4} \tag{C.8}$$

We have to solve this set of four differential equations. We could derive them to remove the integral, but we can leave it and solve the equations with a variable that will evaluate that integral every time step. There are many algorithms for solving differential equations, we will consider one of the simplest, the Taylor series [23] :

$$f(t_{n+1}) = f(t_n) + \Delta t f'(t_n) + (\Delta t)^2 \frac{f''(t_n)}{2} + \dots \tag{C.9}$$

where the time step is $\Delta t = t_{n+1} - t_n$. Equation C.9 up to second order is adapted for equations C.5 to C.8:

$$I(t + \Delta t) = I(t) + \Delta t \cdot I'(t) + \Delta t \frac{I'(t) - I'(t - \Delta t)}{2} \tag{C.10}$$

The implementation of this algorithm in C++ is straight forward and can also be found on GitHub [22]. The program created resulted to be almost a 500% faster than OrCAD performing the same simulation and giving very similar results[21]. The program is much faster because we are not simulating the circuit, but a simplified model.

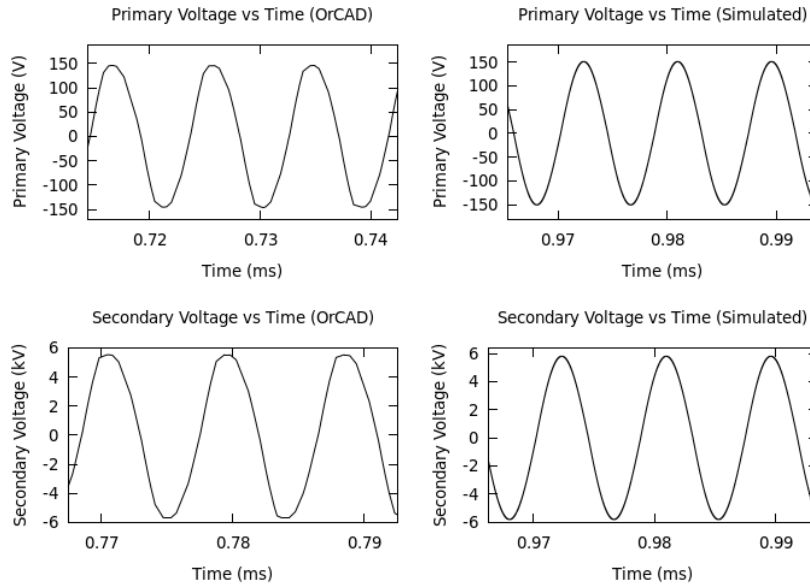
Figure 54: Comparison of results. Time window is again not important (as in figure 5), only voltage and current values, wave shapes and frequency.

---

[21] The code has convergence errors if L1 is too small. More work on this program is needed.

References

[1] James E. Turner,
Atoms, Radiation, and Radiation Protection,
Wiley-VCH, 2007.

[2] CEI OX/70-G4 X-Ray Datasheet,
http://www.ceixray.com/content/uploads/prodotto_image/OX70_G4.pdf

[3] The ZVS Driver
https://www.instructables.com/id/The-ZVS-driver/

[4] TDK Ferrite and accessories, ETD59/31/22
https://www.tdk-electronics.tdk.com/inf/80/db/fer/etd_59_31_22.pdf

[5] Texas Instruments TPS2814P Datasheet
http://www.ti.com/lit/ds/symlink/tps2812.pdf

[6] TDK Ferrite and accessories, SIFERRIT material N87
https://www.tdk-electronics.tdk.com/download/528882/
71e02c7b9384de1331b3f625ce4b2123/pdf-n87.pdf

[7] MeanWell EPP-300-48 Datasheet
https://www.mouser.es/datasheet/2/260/r1835_3-1109476.pdf

[8] Microchip TC4469 Datasheet
http://ww1.microchip.com/downloads/en/DeviceDoc/21425C.pdf

[9] Infineon IR2110 Datasheet
https://www.infineon.com/dgdl/ir2110.pdf?fileId=5546d462533600a4015355c80333167e

[10] Texas Instruments, Understanding Schmitt triggers
http://www.ti.com/lit/an/scea046/scea046.pdf

[11] Texas instruments, Understanding Undervoltage Lockout in Power Devices
http://www.ti.com/lit/an/slva769a/slva769a.pdf

[12] International Rectifier IRFP250N Datasheet
https://docs-emea.rs-online.com/webdocs/0791/0900766b8079120f.pdf

[13] Skin Depth Calculator
https://www.pasternack.com/t-calculator-skin-depth.aspx

[14] Block 0.15mm Datasheet
https://docs-emea.rs-online.com/webdocs/1218/0900766b81218993.pdf

[15] NIST Lead Attenuation Coefficients
https://physics.nist.gov/PhysRefData/XrayMassCoef/ElemTab/z82.html

[16] NISTX Calculator
http://solutioinsilico.com/medical-physics/applications/nist-lookup.php

[17] Slice Reconstruction
http://homepages.inf.ed.ac.uk/rbf/CVonline/LOCAL_COPIES/
AV0405/HAYDEN/Slice_Reconstruction.html

[18] Peter Andual Toft,
The Radon Transform - Theory and Implementation
PhD Thesis, University of Denmark, 1996.

[19] Filtered Back Projection C++ Implementation
https://github.com/fpiernas/FBP

[20] Body Sinogram Example
https://www.podcastscience.fm/ps254_6ffdcfaca9214e08a17cc083b34c1043-jpg/

[21] Helix Pseudocolor Algorithm
https://github.com/fpiernas/HPC

[22] ZVS Mazzilli Driver Simulator
https://github.com/fpiernas/ZVS-Sim

[23] V. Tomeo, I. Uña, J. San Martín,
Cálculo en una variable
Ibergaceta, 2011.

[24] The Physics Hypertextbook
https://physics.info/em-spectrum/

[25] Ned Mohan, Tore M. Undeland, William P. Robbins
Power Electronics: converters, applications and design
John Wiley & Sons, 1995.

[26] Mulutukla S. Sarma
Introduction to Electrical Engineering
Oxford University Press, 2001.

[27] Shepp-Logan Phantom
https://imagej.nih.gov/ij/plugins/radon-transform.html

[28] List of parts, tools and software used
https://docs.google.com/spreadsheets/d/
1ojSCOUx2DOwuFIo_I8m1rTHGgjrr8TNEGdr5XydzT6Q/